Precambrian Research 362 (2021) 106304

Contents lists available at ScienceDirect

Precambrian Research

journal homepage: www.elsevier.com/locate/precamres

Palaeoproterozoic foreland fold-thrust belt structures and lateral faults in the West Troms Basement Complex, northern Norway, and their relation to inverted metasedimentary sequences

Hanne-Kristin Paulsen [a,b,*], Steffen G. Bergh [a,*], Sabina Strmić Palinkaš [a], Siri Elén Karlsen [a], Sofie Kolsum [a], Ida Ulvik Rønningen [a], Paul E.B. Armitage [c], Aziz Nasuti [b]

[a] Department of Geosciences, UiT The Arctic University of Norway, N-9037 Tromsø, Norway
[b] Geological Survey of Norway, N-7491 Trondheim, Norway
[c] Paul Armitage Consulting Ltd, 1 Aster Drive, St Mary's Island, Chatham, ME4 3EB, United Kingdom

ARTICLE INFO

Keywords:
Fold thrust belt
Rift-related sediments
Basin inversion
Late/post Svecofennian
Vanna/Vannøy

ABSTRACT

Palaeoproterozoic fold-thrust belt structures and steep, lateral shear zones characterize the foreland deformation of Neoarchaean basement tonalites in Vanna, West Troms Basement Complex, northern Norway. Low-grade para-autochthonous and allochthonous cover units (2.4–2.2. Ga) with sandstones and calcareous metapelites exist in separate areas of the foreland. They were formed as intracontinental rift- and/or deltaic shelf deposits, and subsequently intruded by a diorite sill at c. 2.2 Ga. The basement and cover units were folded and inverted along low-angle thrusts and steep reverse faults during two late/post Svecofennian (1.77–1.63 Ga) orthogonal shortening events (D_1-D_2). The D_1 event involved NE-SW shortening, folding, ENE-directed thrusting, and dextral lateral shearing, controlled by pre-existing, N-S striking mafic dykes (c. 2.4 Ga) and basin-bounding normal faults. The D_2 event involved SE vergent nappe translation, flat-ramp thrust propagation in a frontal duplex above a basement-seated detachment, and sinistral lateral reactivation in a partitioned orogen-parallel, transpressive setting. Hydrothermal fluid circulation affected all the shear zones. New aeromagnetic data show the basement-involved fold-thrust belt architecture well. The orthogonal Vanna Island fold-thrust belt styles of deformation resemble other inverted rift-basin deposits in northern Fennoscandia, deformed during the Svecofennian Orogeny (1.92–1.79 Ga), Alta-Kautokeino and Karasjok greenstone belts in northern Norway, Central Lapland, Peräpohja, Kittilä and Kuusamo belts of Finland, and in the Norrbotten province of Sweden. Westward younging of the orogenic events explain the younger age span of deformation on Vanna Island.

1. Introduction

Foreland fold-thrust belts are the most common way to accommodate crustal shortening in frontal parts of orogens. Such belts are worldwide distributed, typically involve basement rocks and overlying sedimentary cover rocks deposited in rift- and/or shelf basins of former continental margins, and have formed in time span from the Archaean to present (Poblet and Lisle, 2011). Pre-existing basin geometries and zones of weakness in the crust, e.g., bounding extensional faults, may control the geometry, structural style, and evolution of a fold-thrust belt during basin inversion (e.g. Gillcrist et al., 1987; Bond and McClay, 1995; Corfield et al., 1996; Butler et al., 2018), whether the deformation is thin- or thick skinned (Butler et al., 2006), and/or if deformation occurred along mechanically weak detachment zones (Homberg et al., 2002). In a metallogenetic perspective, large-scale basement-seated ductile shear zones may act as conduits for deep crustal fluids that are important for forming ore-deposits (Cox, 2005; Bauer et al., 2014). Thus, the study of basement cover relationships in foreland fold-thrust belts is fundamental to resolving the ore potential in such settings. The study of Archaean and Proterozoic fold-thrust belts, however, is hindered by the low preservation potential, since commonly only the deeply eroded core parts remain.

The interior parts of the Fennoscandian Shield (northern Finland and Sweden) are a good example where the boundary conditions between Archaean and Palaeoproterozoic rocks and fold-thrust belt architectures are deeply eroded and hence field and geophysical studies addressing

* Corresponding authors at: Department of Geosciences, UiT The Arctic University of Norway, N-9037 Tromsø, Norway (H.-K. Paulsen).
E-mail addresses: hanne-kristin.paulsen@ngu.no (H.-K. Paulsen), steffen.bergh@uit.no (S.G. Bergh).

https://doi.org/10.1016/j.precamres.2021.106304
Received 28 January 2021; Received in revised form 3 June 2021; Accepted 4 June 2021
Available online 15 July 2021

the basement-cover linkages are few (e.g. Piippo et al., 2019; Lahtinen and Köykkä, 2020). By contrast, basement provinces on the northwest margin of the Fennoscandian shield in northern Norway expose many low-metamorphic grade sections of fold-thrust belts (cf. Bergh et al., 2010, 2015), and admit perhaps a more detailed image of upper crustal architectures and control on mineralization than most studies in the Fennoscandian Shield can achieve. The West Troms Basement Complex (WTBC) is contiguous with the Fennoscandian shield but situated west of the Palaeozoic Scandinavian Caledonides (Fig. 1; Gorbatschev and Bogdanova, 1993; Hölttä et al., 2008; Lahtinen et al., 2005, 2009, 2015). This province allows regional-scale studies of a presumed late-/post Svecofennian and/or early Gothian (1.77–1.63 Ga) accretionary orogen and its long-lasting tectono-magmatic history (Bergh et al., 2010, 2015). The WTBC hosts Neoarchaean and Palaeoproterozoic basement tonalities and gneisses preserved in a mid- to upper crustal transect (Fig. 2; Bergh et al., 2010; Myhre et al., 2013; Laurent et al., 2019). The upper crustal portion of this transect is exposed in the northeast (Vanna Island), comprising a foreland basement-involved fold-thrust belt system with inverted Palaeoproterozoic metasedimentary sequences (Figs. 2, 3).

This paper introduces new data on pre-orogenic extensional basins (2.4–2.2 Ga) and late/post Svecofennian compressional and strike-slip structures (1.77–1.63 Ga) and discusses the evolution of the Vanna Island fold-thrust belt using field data and aero-magnetic susceptibility data (Nasuti et al., 2015; Sandstad, 2015). We focus on the Neoarchaean basement rocks and several overlying Palaeoproterozoic cover/basin sequences, now preserved as par-autochtonous and allochthonous units. To resolve the basin architectures and depositional regime, we compared and correlated the internal stratigraphy and depositional history of the previously described par-autochthonous Vanna Group (Bergh et al., 2007) with selected new areas of the Vanna foreland, at Larstangen-Myra in the southeast (Figs. 3, 4), and at Hamre-Kvalvågklubben in the west (Fig. 3). In addition, we describe the Svartbergan Nappe, a recently uncovered > 500 m thick allochthonous series of steeply tilted quartzites and metapelites below the Skipsfjord Nappe and above a major frontal ductile thrust system (Fig. 3). We then characterised the fold-thrust belt style deformation in the different areas and linked them to map-scale fold patterns and basement-seated deformation zones, and further evaluated if the resulting orogenic structures were linked to inherited basement discontinuities. The data show that the basement and individual cover units responded to inversion by two-stage (D_1-D_2), orthogonal crustal shortening and lateral shearing events. We further argue that the extent and geometry of the pre-existing basin units, their boundary normal faults, and an associated 2.4 Ga dyke swarm (Kullerud et al., 2006), may have controlled inversion that resulted in folding and thrust propagation above basement-seated detachments, as well as hydrothermal alteration and quartz-carbonate precipitation in thrusts and strike-slip shear zones (Paulsen, 2019). Finally, we compare the foreland structural pattern of Vanna Island with hinterland structures farther southwest in the WTBC, and address links to inverted fold-thrust belt settings elsewhere in the Fennoscandian Shield.

2. Geological setting

2.1. Regional framework

The northern Fennoscandian Shield evolved through multiple Archaean (2.7–2.6 Ga) and Palaeoproterozoic rifting (2.5–1.9 Ga) and collisional orogenic events, such as the Lapland-Kola (1.94–1.86 Ga), Svecofennian (1.92–1.79 Ga), and Gothian (c.1.6 Ga) orogenies, resulting in the amalgamation of an Archaean nuclei in the northeast and widespread Palaeoproterozoic accretionary growth towards the southwest (e.g. Kärki et al., 1993; Nironen, 1997; Lahtinen et al., 2005;

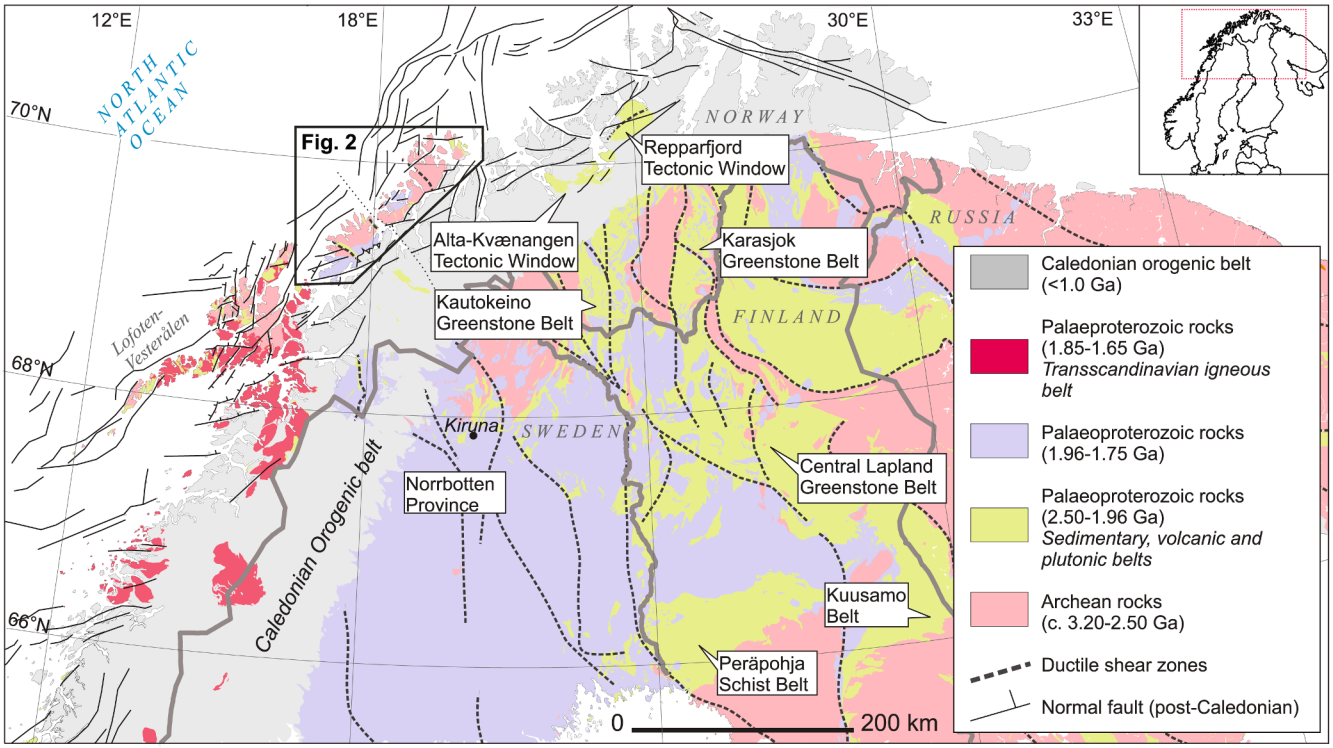

Fig. 1. Regional geological map of the northern Fennoscandian Shield based on Koistinen et al., (2001), Olesen et al., (2002), Eilu et al., (2008) and Bergh et al., (2010). Basement provinces include the West Troms Basement Complex (outlined by the black frame; Fig. 2) and the Lofoten-Vesterålen area to the west of the Caledonian Orogenic belt, Repparfjord, and Alta-Kvænangen supracrustal units in tectonic windows, and the Karasjok, Kautokeino and Central Lapland greenstone belts, Peräpohja Schist Belt, Kuusamo Belt and Norrbotten Province east of the Caledonides. Note a general N-S to NW-SE trend of Palaeoproterozoic supracrustal belts and major ductile shear zones.

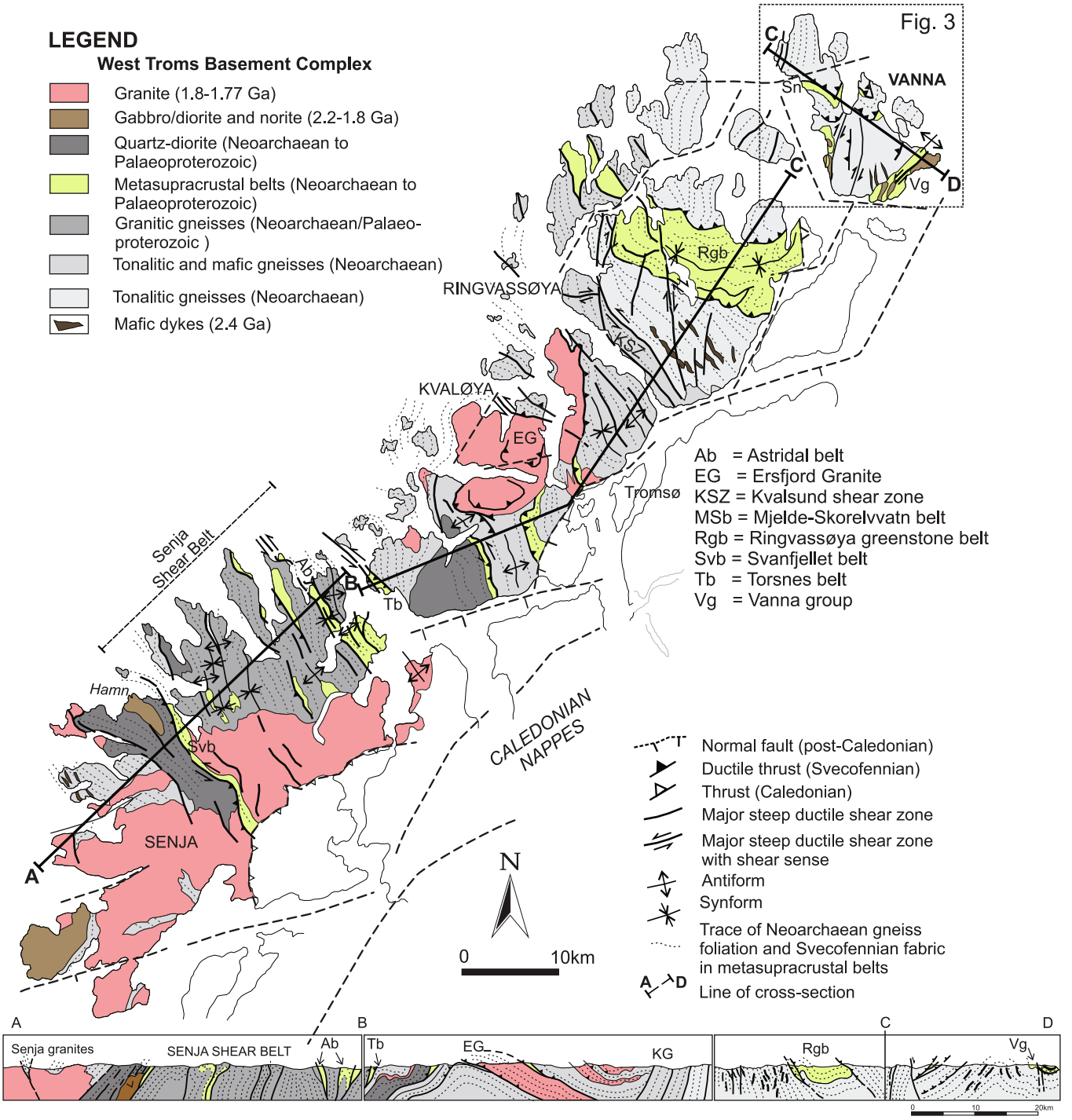

Fig. 2. Geologic-tectonic map and cross-section of the West Troms Basement Complex (modified after Kullerud et al., 2006; Bergh et al., 2007, 2010). Vanna Island is in the northern part of the complex and is outlined with a black frame (Fig. 3).

Daly et al., 2006; Åhäll and Connelly, 2008). In the northeast (Fig. 1), Archaean basement gneisses are overlain by Palaeoproterozoic volcano-sedimentary shelf and rift-basin deposits formed during a period of major crustal extension (Lahtinen et al., 2008; Bingen et al., 2015; Lahtinen and Köykkä, 2020). Rifting initiated by c. 2.45 Ga mafic intrusions (Huhma et al., 2018), followed by break-up at c. 2.1 Ga (Bingen et al., 2015) of e.g. the Karelian and Norrbotten cratons (Fig. 1), with formation of rift-basins and internal shelf- and passive margin basins with thick greywacke and turbiditic deposits (Bingen et al., 2015; Lahtinen and Köykkä, 2020). During the Lapland-Kola and Svecofennian orogenies the basins in between the Karelian and Norrbotten blocks closed by arc-accretion, subduction, and continent–continent collision (Gaàl and Gorbatschev, 1987; Nironen, 1997; Korsman et al., 1997; Cagnard et al., 2007; Lahtinen et al., 2008, 2009). Foreland fold-thrust belts formed in the Central Lapland and Kuusamo belts at age frames between c. 1.93–1.91 Ga (Daly et al., 2006; Lahtinen and Köykkä, 2020), at c. 1.88–1.87 Ga in the Kiruna area (Piippo et al., 2019; Andersson et al., 2020), and post-1.8 Ga due to shortening in back-arc related volcanic rocks (Lahtinen et al., 2018).

Archaean and Palaeoproterozoic basement-cover rocks also exist in tectonic windows and northwest of the Palaeozoic Scandinavian Caledonides in northern Norway (Fig. 1). Examples are the Alta- Kautokeino

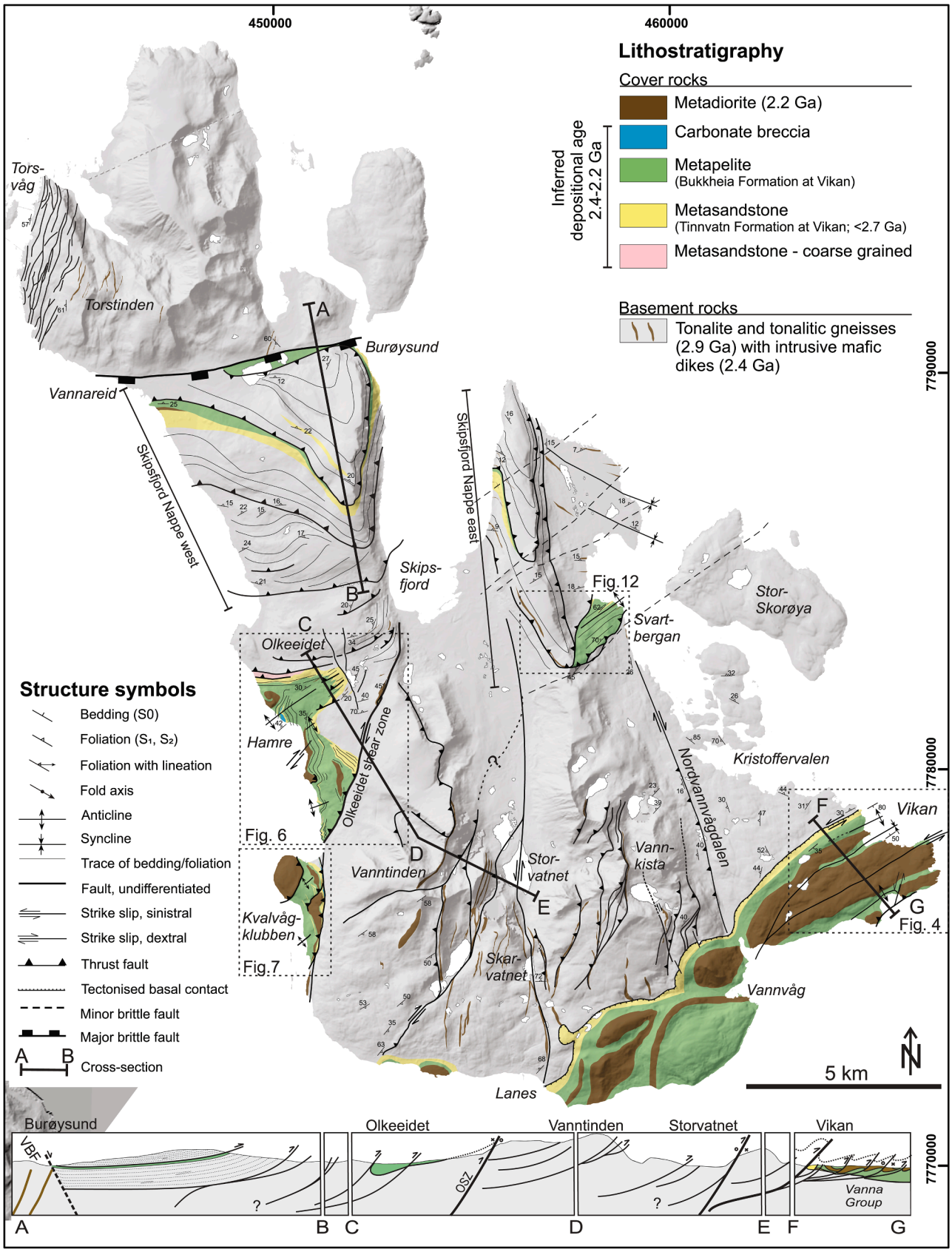

Fig. 3. Geologic-tectonic map and interpreted, composite cross-section A-G of Vanna island, modified after Bergh et al., (2007) and Opheim and Andresen, (1989). The areas of metasedimentary cover sequences mapped in detail are outlined with black stippled frames: southeastern foreland at Vikan-Larstangen (Vanna Group; Fig. 4), western foreland units: Hamre (Fig. 6), Kvalvågklubben (Fig. 7), Skipsfjord Nappe, and Svartbergan Nappe (Fig. 12).

and Karasjok greenstone belts in Finnmark (Fig. 1), correlative with the Central Lapland and Norrbotten provinces in Finland and northern Sweden (Braathen and Davidsen, 2000; Hanski and Huhma, 2005; Bingen et al., 2015; Melezhik et al., 2015b). The WTBC and corresponding Lofoten-Vesterålen plutonic suite crop out southwest of the Caledonides (Griffin et al., 1978; Corfu, 2004, 2007), but are interpreted as a part of the Fennoscandian Shield (Bergh et al., 2010, 2012; Henderson et al., 2015; Skyttä et al., 2020). The oldest rocks in the WTBC are Meso- and Neoarchaean tonalitic, granitoid and dioritic (TTG) gneisses and migmatites (2.9–2.6 Ga; Bergh et al., 2010; Myhre et al., 2013; Laurent et al., 2019), deformed during Neoarchaean orogenies (2.8–2.6 Ga; Myhre et al., 2013), and spatially separated by lens-shaped ductile shear zones (Bergh et al., 2010). Later, an extensive mafic dyke swarm dated at c. 2.4 Ga intruded the basement gneisses (Kullerud et al., 2006), and sedimentary cover units were deposited on top of the gneisses (Armitage and Bergh, 2005; Bergh et al., 2010). Depositional ages span from c. 2.7 Ga for the Ringvassøya greenstone belt (Zwaan, 1989; Motuza, 2000), via a 2.4–2.2 Ga age for the low-grade Vanna Group (this work) (Bergh et al., 2007), to > 1.9 Ga for the Torsnes supracrustal rocks (Myhre, 2011). Granitoid and mafic plutonic rocks (c. 1.8 Ga) formed in central and southern parts of the WTBC (Fig. 2; Corfu et al., 2003; Bergh et al., 2010; Laurent et al., 2019) synchronous with plutonic rocks in Lofoten and Vesterålen (Corfu, 2004). These arc-related plutonic rocks marked the onset of a major orogenic event in the WTBC, with a tentative age span of 1.77–1.63 Ga (Corfu et al., 2003; Bergh et al., 2015), reflecting the late/post-stages of the Svecofennian orogeny, or the Gothian orogeny, as defined in Fennoscandia (Lahtinen et al., 2008).

This orogenic deformation affected the entire WTBC by an early NE-SW shortening event, dated at c. 1.77–1.75 Ga in the Senja shear belt (Bergh et al., 2015), where characteristic deformation structures include recumbent folds, a main foliation and SW- and NE-dipping thrusts, and subsequent coaxial, NW-SE-trending upright macroscopic folds (Bergh et al., 2010). During a later partitioned transpressional event at c. 1.75–1.63 Ga (Bergh et al., 2015) NW-SE trending subvertical folds and steep, orogen-oblique (N-S) strike-slip shear zones formed in the Senja Shear Belt, whereas SE-directed (orogen-parallel) thrusts and NW-SE trending lateral shear zones formed on Vanna Island, within the northeastern part of the WTBC (this work; Fig. 2; Bergh et al., 2007, 2010). Peak metamorphism reached high- and medium grade in the Lofoten-Vesterålen and Senja parts of the transect (Fig. 1) during the early event, whereas low-grade conditions characterized the later events in Vanna Island. The data imply that the transect (Fig. 2) evolved from an arc-magmatic hinterland with subduction toward the SW (deep crust) in the southwest, to the studied foreland fold-thrust belt system (upper crust) in the northeast on Vanna Island (Bergh et al., 2010).

2.2. Vanna foreland

The foreland part of the WTBC on Vanna Island (Fig. 2) exposes Neoarchaean tonalitic basement (c. 2.9 Ga) intruded by inferred 2.4 Ga mafic dykes (Kullerud et al., 2006), and overlying, low-grade metasedimentary cover sequences (Fig. 3; Binns et al., 1980; Johansen, 1987; Bergh et al., 2007). Previously studied cover units (Fig. 3) are the low-grade, par-autochtonous Vanna Group overlying basement tonalites at Vikan in the southeast (Binns et al., 1980; Bergh et al., 2007), and dismembered units in allochthonous basement rocks of the Skipsfjord Nappe in the northwest (Opheim and Andresen, 1989). In addition, unexplored, par-autochtonous sedimentary units exist in the west at Hamre and Kvalvågklubben and as allochthonous units at Svartbergan in the east (Fig. 3, this work). Comparison of the internal stratigraphy and sedimentary characteristics, and basement-cover contacts of these cover units with those at Vikan is critical when trying to restore the overall basin architectures.

The low-grade metasedimentary Vanna Group unconformably overlies Neoarchaean tonalites along a steep, folded basement-cover contact (Fig. 4). The Vanna Group starts with a 20 cm thick basal conglomerate (Bergh et al., 2007), followed by a c. 70 m thick sequence of arkosic sandstones (Tinnvatn Formation) with well-sorted rhythmic lamination and channel structures indicating shallow marine, high-energy deltaic or tidal, shore-face deposits (Binns et al., 1980; Bergh et al., 2007). Palaeocurrent data yielded transport directions of deltaic streams along NNE-SSW and NNW-SSE trending axes, or presumed coastlines (Johannessen, 2012). The Tinnvatn Formation is overlain by a c. 100 m thick calcareous mud- and siltstone sequence (Bukkheia Formation) displaying ripple and mud cracks indicating tidal marine deposition (Binns et al., 1980). In its uppermost part, this formation is intruded by a diorite sill dated at 2221 ± 3 Ma (Bergh et al., 2007), which is a minimum age for the Vanna Group rocks, whereas a 2.4 Ga mafic dyke swarm in the underlying basement rocks does not penetrate the cover contact, thus yield a maximum age for the Vanna Group. These ages revoked a previously interpreted Neoproterozoic depositional age (Binns et al., 1980). Detrital zircon ages in the Tinnvatn Formation (Bergh et al., 2007) indicate a provenance (2.9–2.7 Ga) from the adjacent Neoarchaean basement tonalites (Fig. 3). Structurally, the entire Vanna Group and diorite sill at Vikan are folded by major SE-verging, asymmetric folds with associated NW-dipping axial-planar foliation and thrust faults (Fig. 4a, b). Ductile thrusts repeat the stratigraphy of the Bukkheia mudstones and define the contact to the Tinnvatn Formation. In addition, younger subvertical folds refolded the tilted metasandstone beds, creating a set of steep W-E striking sinistral strike-slip shear zones (Fig. 4c).

The Skipsfjord Nappe in the north-central part of Vanna Island (Fig. 3) is an allochthonous thrust nappe with several larger sheets of mylonitized tonalitic basement gneisses and lenses of metasedimentary and mafic intrusive rocks (Opheim and Andresen, 1989). The metasedimentary sequence is < 100 m thick and has tectonized contacts. It is more highly strained than other cover units on Vanna Island, although the metamorphic grade never exceeded greenschist facies. Opheim and Andresen (1989) divided the sequence into a lower unit of metasandstones and an upper unit of calcareous metapelites and siltstones, thus indicating a similar build-up as for the Vanna Group. The main tectonic feature of the Skipsfjord Nappe rocks is a gently NW-dipping mylonitic foliation, which is locally irregular due to the presence of less deformed, foliation-parallel tonalite lenses, mafic intrusive sills, and numerous secondary carbonate and quartz veins.

The southern contact of the Skipsfjord Nappe is constrained to a major frontal ductile thrust system below the Svartbergan Nappe, a > 500 m thick allochthonous series of steeply tilted quartzites and metapelites (Fig. 3). The northern boundary of the Skipsfjord Nappe is the Permian-aged Vannareid-Burøysund fault (Davids et al., 2013), which down-faulted the nappe > 3 km to the south (Opheim and Andresen, 1989). This brittle fault comprises widespread Cu-Zn bearing hydrothermal quartz-carbonate deposits thought to be controlled by the underlying basement-structures along the contact (Paulsen et al., 2020).

3. Methods and data

The present study builds on previous published data (e.g. Binns et al., 1980; Opheim and Andresen, 1989; Bergh et al., 2007) and new regional field and structural data collected. These new field data include the work of three master students that also contributed to this study (Karlsen, 2019; Kolsum, 2019; Rønningen, 2019). Detailed geological maps were compiled from four key areas on Vanna Island (Fig. 3) including: (i) the par-autochtonous Vanna Group at Larstangen and Myra in the southeastern foreland, (ii) the western foreland at Hamre and Kvalvågklubben (for comparison with the Vanna Group), and (iii) allochthonous basement and cover units of the Svartbergan Nappe in north-central Vanna Island. Litho-stratigraphic columns and sedimentological data were gathered from each of the areas as basis for correlation of the cover units.

Detailed structural mapping and analysis were conducted in all the mentioned key areas, both in basement tonalites, par-autochthonous

and allochthonous sedimentary cover rocks, and along their contacts. We address relations of bedding and foliation data, macro- and *meso*-scale folds, ductile shear zones, and kinematic characters, and relative timing of cross-cutting fabrics. The term 'foliation' is used for the main planar fabric of the bedrocks, formed as different generations of fold axial-planar and subsidiary planar fabrics in the southeastern foreland area (D_2), western foreland areas (D_1), and in the Skipsfjord Nappe rocks (D_2), respectively. Stretching and mineral lineations generally overlap in orientation and are associated with ductile shear zones, and thus, both are considered a result of ductile shearing (D_1 or D_2). Notably, we evaluated if orogenic structures in the cover units were linked to inherited basement discontinuities, pre-existing extensional faults, intrusive mafic dykes, and/or basement-seated detachments. The new structural data (> 1000 readings) were integrated between the studied areas to link a prevalent pattern of basement and cover structures into a wider framework. The results allowed us to argue for the two-phased orthogonal (D_1-D_2) basement-involved fold-thrust belt deformation, and to discuss the controlling effect of basement structures, mafic dykes, and basin-boundary normal faults on inversion of the cover sequences.

Reprocessed magnetic data (Rodionov and Ofstad, 2012; Nasuti et al., 2015; Sandstad, 2015) were used to test our field data and resolve the foreland structural architecture of Vanna Island. We interpreted data sets converted to total magnetic and tilt derivative fields using the methods of Henkel (1991), then referenced all previous bedrock geology knowledge, and validated the interpretations. In particular, the magnetic data were useful to interpret the structural fabrics in basement tonalites in areas with steep topography and Quaternary overburden.

4. Results

4.1. Components of the southeastern foreland units (Vanna Group)

The Vanna Group and its relation to diorite sills and fold-thrust belt structures is previously described at Vikan and Skippervika (Fig. 4a-c; Bergh et al., 2007). Data from Larstangen show that bedding in Bukkheia Formation metapelites is conformable with the intrusive diorite contacts (Fig. 4d) and a strong mylonitic foliation dipping moderately to the WNW (Fig. 4e), and with stretched calcareous clasts plunging NW to WNW (Fig. 4e, 5a, b). Bedding in mudstones at Myra is folded by E-W trending isoclinal folds with a main axial-planar mylonitic foliation, then refolded coaxially, by tight upright E-W trending folds with stretching lineations parallel to fold axes (Fig. 4f, 5c). Gently northwest-dipping thrust zones with stretched clasts are also folded by the later upright folds (Fig. 5b), and new, NNW-SSE striking mylonitic lateral (strike-slip) shear zones are developed along the steep axial surface of such folds (Fig. 4g).

The massive diorite sill at Myra is folded together with the metapelites and accommodated ductile shearing along the diorite-sediment contact and inside the diorite itself (Fig. 4). The contact is marked by a 5–10 m thick zone of mylonitized mudstones and calcareous mafic schists. A similar, but thicker (c.20 m) high-strain zone in the diorite contains an irregular NW-dipping mylonitic foliation wrapped around sigmoidal lenses of massive diorite (Fig. 5d), and with dip-slip stretching lineations plunging NW (Fig. 4h). This shear zone formed along the axial-surfaces of asymmetric, SE-verging folds in mega-lenses (> 5 m thick) of metasandstones (Fig. 5e), interpreted as xenoliths in the diorite, thus demonstrating SE-vergent folding and thrusting. Presence of hydrothermal carbonate and quartz-rich veins, sulphides, and secondary epidote, chlorite, and adularia in all the diorite-internal thrust and steep lateral shear zones (e.g. Fig. 5f) indicate widespread hydrothermal fluid circulation synchronous with the fold-thrust deformation.

4.2. Components of the western foreland cover units

Metasedimentary cover sequences are also present on the western side of Vanna Island, between Hamre and Kvalvågklubben (Fig. 3), bounded in the north by the Skipsfjord Nappe and in the east partly by the steeply west-dipping Olkeeidet shear zone. Detailed mapping (Figs. 6, 7) shows a basal metasandstone series (< 200 m thick) dipping moderately SW (Fig. 8a, b), and a conformably overlying upper series of metapelites with embedded diorite lenses/sills > 100 m thick. Cross-beds in the metasandstones (Fig. 8c) indicate the strata are right-way-up. The transition to the conformably overlying metapelites is a peculiar, calcareous breccia (c. 50 m thick) with angular fragments of mudstone embedded in a calcite-dolomite matrix (Fig. 8d), used as a tectono-stratigraphic marker. Stratigraphic-internal thickness changes are hard to detect due to rather complex deformation (see below), but an increase in thickness of the metasandstones eastward toward the boundary fault is apparent (Fig. 6).

Structurally, the entire metasedimentary sequence strikes c. N-S in the south and becomes gradually folded around an ENE-WSW trending axial trace in the north (Figs. 6, 7, and stereonets) near the NW-dipping frontal thrust sheets of the Skipsfjord Nappe (Fig. 6; cross-section A-A', 8a). When present, primary bedding is steep E- or W-dipping (Fig. 9a) possibly as part of an asymmetric, ENE-vergent fold limb (D_1), e.g., at Kvalen (Fig. 7). In petapelites, however, primary bedding is mostly obliterated by a gently WSW-dipping penetrative foliation (D_1) (Fig. 9a). This main foliation is axial-planar to tight isoclinal, ENE-verging folds (Fig. 9b) and also parallel to thrusts (D_1) with a moderate dip to the WSW (Figs. 6, 7; stereonets). An example is a ductile thrust in the metapelites at Finneset that emplaces strata ENE-wards on top of steeply tilted metasandstone beds (Fig. 9c). This thrust zone comprises metre-thick quartz-carbonate breccias tightly folded and transposed into the shear zone foliation (Fig. 9d). Shear-zone internal contractional duplexes, sigmoidal lenses, and stretching lineations (Fig. 9e) yield mostly top-to-ENE movement. Some scatter is observed for stretching lineations, indicating oblique dextral thrusting to the NE and NNE (Fig. 7). Similar WNW-dipping thrust zones and kinematic data exist in the diorites (Fig. 9f).

Most mesoscale thrusts and the main foliation in the metapelites are subparallel to a well-exposed boundary fault east of the metasedimentary sequence (Figs. 6, 7). This boundary fault is a steep to moderately west-dipping ductile shear zone (Olkeeidet shear zone) with kinematic data indicating dip-slip thrusting to the ENE and dextral strike-slip movements from drag folding of adjacent strata. Despite its location adjacent to the metasedimentary units, no kinematic evidence for normal fault motion is observed in the bounding faults. In the south (Fig. 7) the Olkeeidet shear zone contains > 30 m thick hydrothermal quartz-carbonate breccias (Fig. 10a, b), with foliation-parallel carbonate separated by layers of green muscovite-fuchsite, and numerous quartz veins (Fig. 10c). Comparable breccias and hydrothermal minerals exist along strike, and inside shear zones in the metasedimentary units and diorites (Fig. 10d-f). The steepest shear zones are narrow, localized (< 5 m wide), c. N-S trending and mostly strike-parallel to the low-angle thrusts. Some merge into each other, and display internal mylonitic fabrics with transposed lenses, subvertical isoclinal folds and asymmetric lenses, recording both reverse movement to the east and dextral strike-slip lateral shearing (Fig. 10e, f).

The superimposed folding (D_2) of the metasedimentary units is well demonstrated in the north (Fig. 6), where the N-S trending D_1 foliation and the basement-cover contact, are affected by a macroscale tight, SE-verging and partly overturned anticlinal fold system. NW-dipping thrust faults (D_2) are also present along the contacts with internal diorite bodies both in the north (Fig. 6; at Hamreklubben and Svartneset) and in the south (Fig. 7; at Straumsnes and Storlikollen), accounting for NW-SE shortening and SE-ward displacement.

4.3. Components of the Svartbergan Nappe

The Svartbergan Nappe defines an allochthonous wedge or mega-lens tectonically below the Skipsfjord Nappe (Figs. 11, 12), with a steep NW-dipping thrust contact to the tonalitic basement (Fig. 12c).

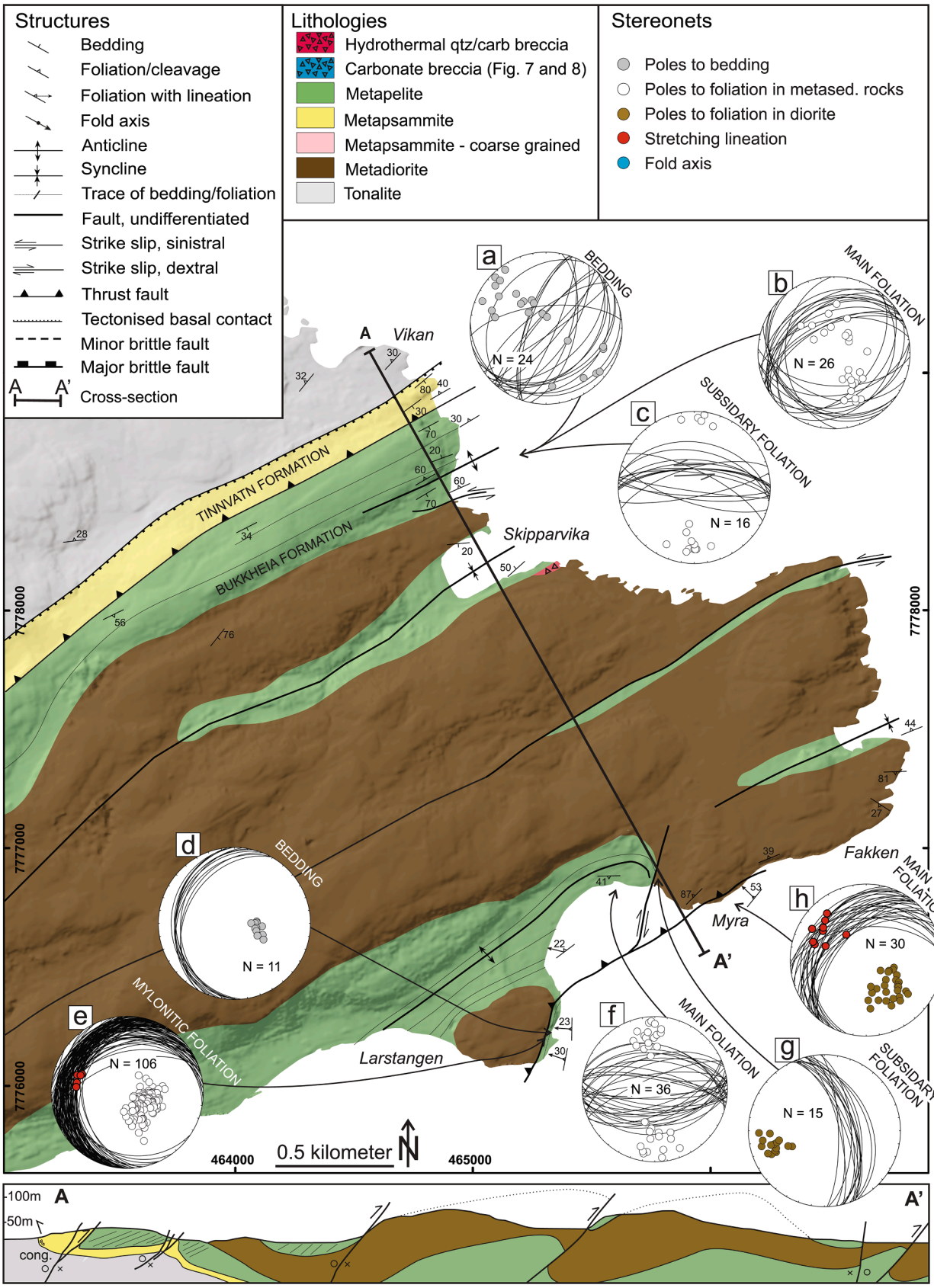

Fig. 4. Geological and structural map with interpreted cross section (A-A') of the southeastern foreland units on Vanna (Bergh et al., 2007). Data in a, b and c are from (Bergh et al., 2007; Pettersen, 2007; Knudsen, 2007). Equal-area lower hemisphere stereonets (a-h) show great circles and poles to bedding and foliation, respectively, and stretching lineations. For location see Fig. 3.

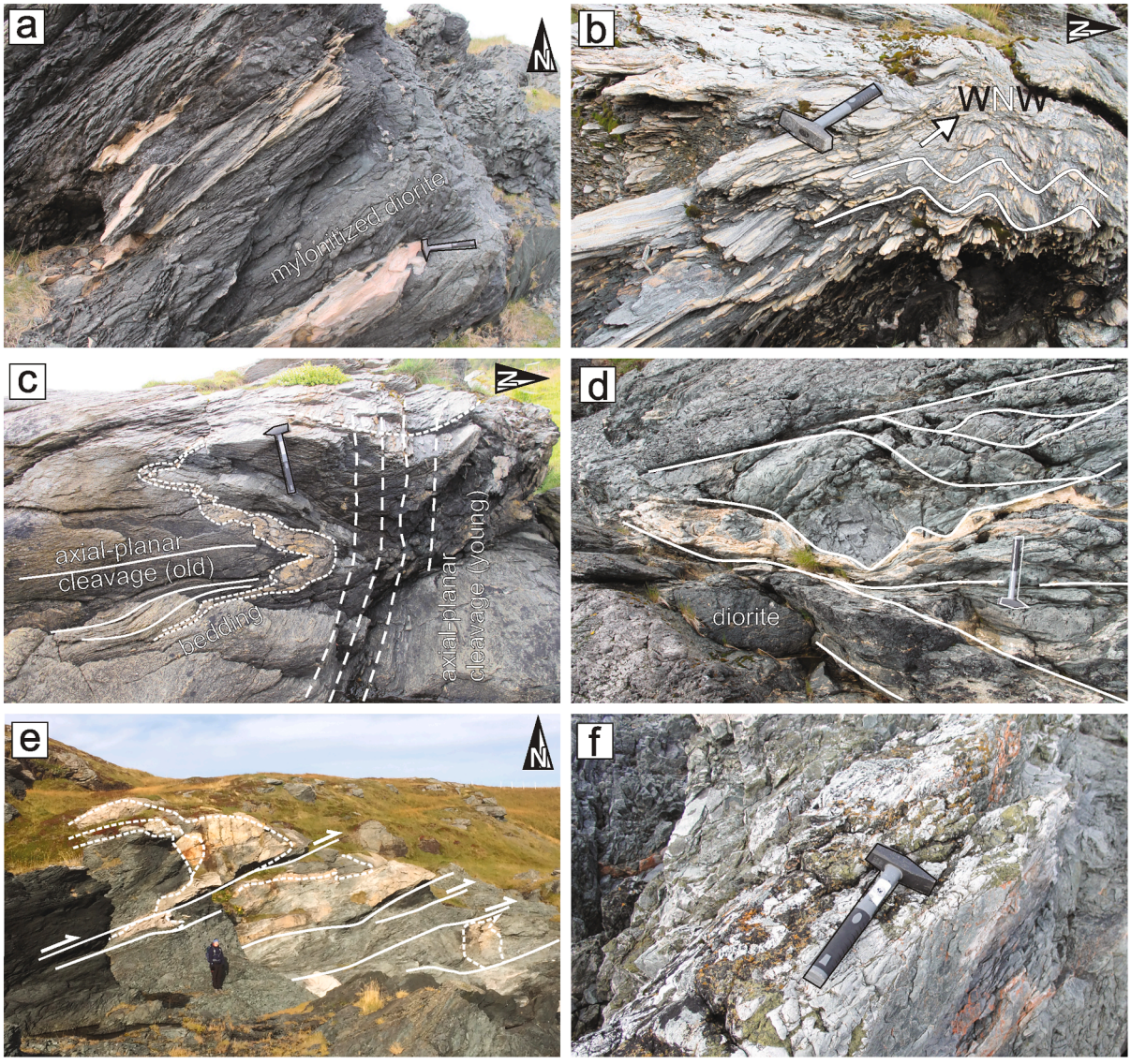

Fig. 5. Outcrop photographs of structures in the southeastern foreland units at Myra and Larstangen (see Fig. 4). a) Mylonitized dark grey diorite at contact with metasandstones. Note lenses of pale metasandstone parallel with mylonite fabric. b) Rodding of sandstone layers yielding a stretching lineation in metapelites, folded by E-W trending upright folds. c) Metapelites with bedding (stippled lines) folded by tight E-W trending isoclinal folds with an axial-planar mylonitic foliation. This foliation is refolded by upright E-W trending folds with subvertical axial surface (long stippled lines). d) Internal anastomosing mylonite zones in diorite form around lenses of massive diorite. Hydrothermal carbonate (pale yellow colour) is common in these zones. e) SE-directed thrusting is indicated by transposed lenses of metasandstone xenoliths in mylonite zone within diorite body. Note person for scale. f) Hydrothermal quartz, carbonate (white) and adularia (red) associated with chlorite (dark green), epidote (bright green) and sulphides are common in the diorite sill. Note hammer for scale.

Internally, this nappe unit has minor thrusts and a main foliation (D_2) conformable with steeply dipping beds of alternating quartzitic metasandstone and muscovite-rich schists (Fig. 13a). Intercalated thin sheets and boudinaged lenses of massive tonalite and granite (Fig. 13b) exist and may be tectonically transposed remnants of the underlying basement rocks. The main foliation dips moderately to steeply (50-80°) to the NW (Fig. 12b), locally to the SE, and consists of low-grade muscovite ± biotite in felsic rocks and amphibole + chlorite + epidote in mafic rocks. The strong mylonitic fabric of these thrusts strikes parallel to the axial surface of transposed, isoclinal folds, and also includes a dip-slip stretching lineation (D_2) plunging variably NW-SE (Fig. 12b), and which is perpendicular to *meso*-scale fold axes.

On a larger scale, the steep NW dip of bedding and foliation in the Svartbergan Nappe rocks may be due to location on a SE-verging D_2 fold limb that is inverted and cut by an overlying thrust (Fig. 12; cross-section A-A'). Such a fold, however, is not confirmed by the field studies. On the mesoscale, asymmetric kink folds trending NE-SW and often displaying opposite SE and NW vergence with conjugate kink bands and cross-cutting crenulation cleavages (Fig. 13c, d). Such kink folds are prevalent and fold the steep foliation/layers and enclosed stretching lineations (Fig. 12b), in contrast to the foliation and stretching lineations in the Skipsfjord Nappe (Fig. 12a). These kink folds/bands indicate continued NW-SE directed D_2 shortening strain (Fig. 12b) relative to the tilting and thrusting event.

The upper contact with the Skipsfjord Nappe is a < 20 m thick transition zone with repeated planar-foliated proto-, ortho-, and ultramylonitic rocks (Fig. 13e), including mylonitic tonalites and quartz-feldspathic calcareous schists. A marked gradual shallowing of the steep NW-dipping foliation in the lower part of the Svartbergan Nappe to c. 30° dip is apparent close to the overlying Skipsfjord Nappe (Fig. 12a). The schists in the transition zone are more extensively sheared and kink-folded compared to rocks in Svartbergan Nappe below (Fig. 13d), thus indicating strain increase upwards (see discussion).

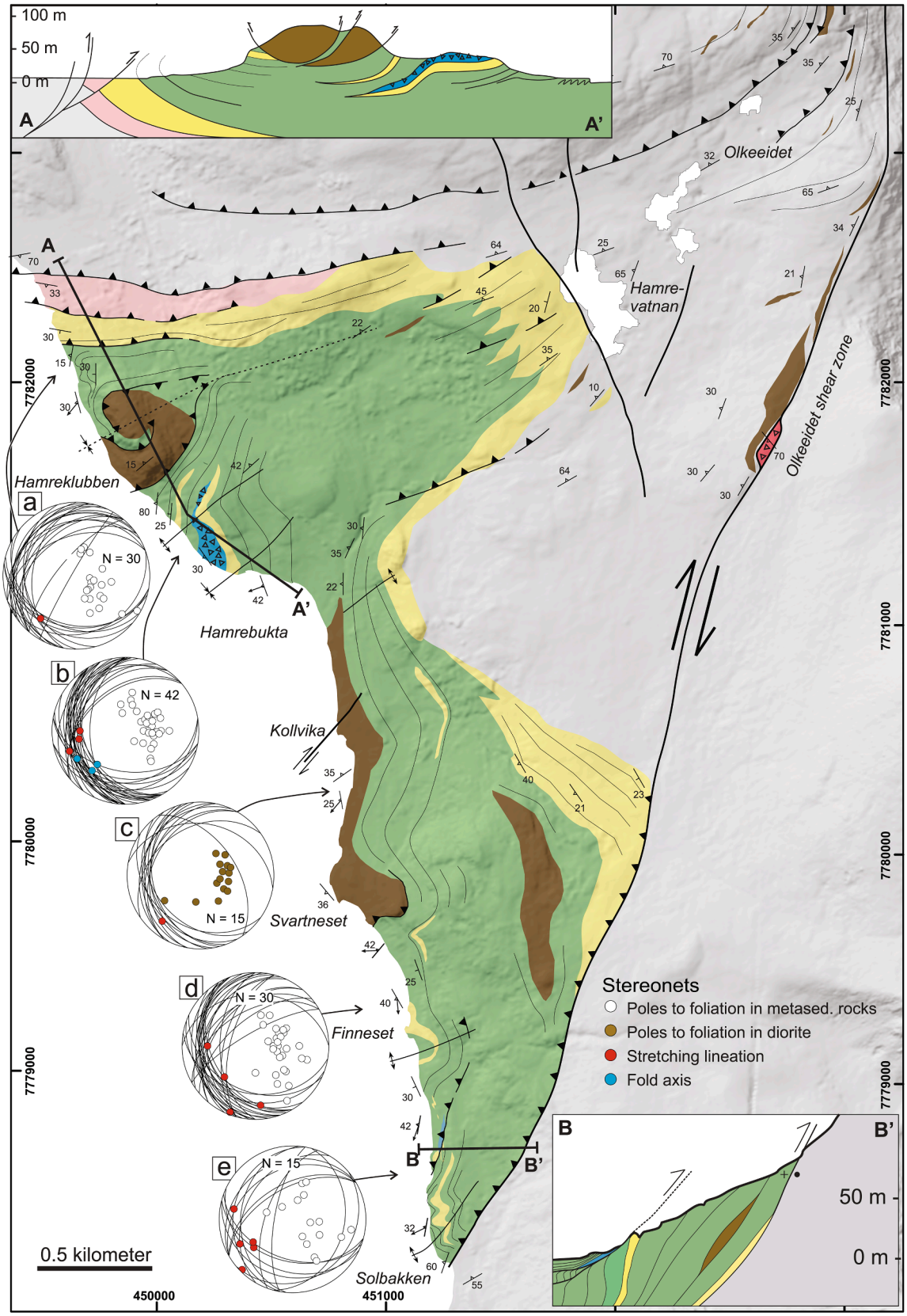

Fig. 6. Geological and structural map of the western foreland units at Hamre. Legend as in Fig. 4. Cross-section A-A' shows coastal transect illustrating the basement-cover contact cut by a thrust fault. Cross-section B-B' traverses the metasedimentary sequence to the steep thrust contact with basement tonalites to the east (Olkeeidet shear zone). Equal-area lower hemisphere stereonets (a-e) showing great circles and poles to foliation, stretching lineations, and measured fold axes. For location of map see Fig. 3.

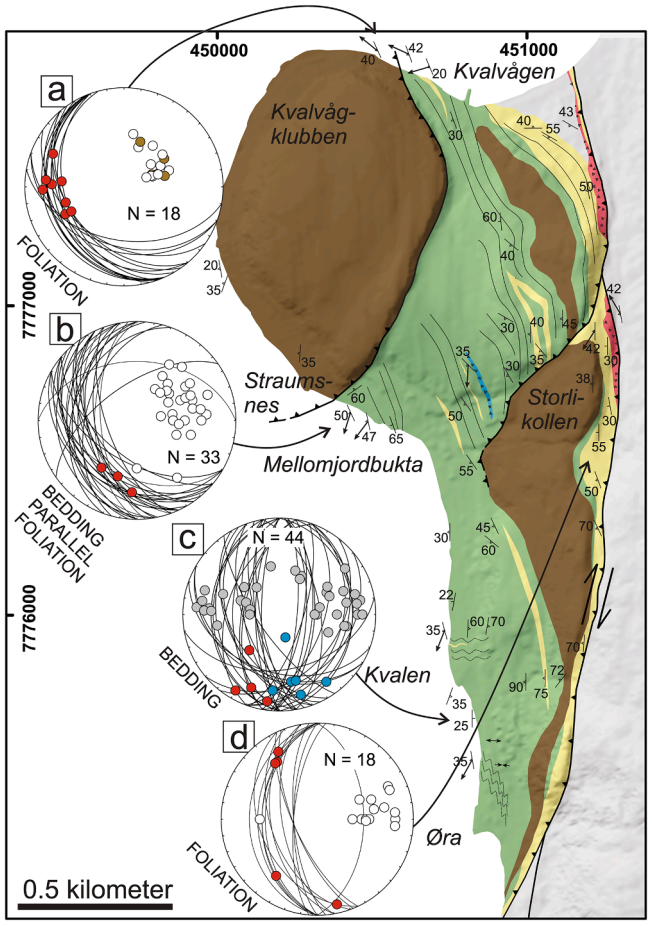

Fig. 7. Geological and structural map of the western foreland units at Kvalvågklubben. Legend as in Fig. 4. Equal-area lower hemisphere stereonets (a-d) show great circles and poles to bedding and foliation, stretching lineations, and measured fold axes. Bedding is commonly foliation parallel. For location of map see Fig. 3.

4.4. Components of basement rocks in southern Vanna Island

Both low- and high-angle mylonitic ductile shear zones are common in the massive basement tonalites in southern Vanna Island (Fig. 14a-h). The low-angle shear zones are striking parallel to a weak N-S to NNW-SSE trending bench fabric and/or composite weak gneiss banding/foliation forming m-scale step-like ledges with a moderate dip to the west. The bench fabric and low-angle shear zones are also parallel to mafic dykes with moderate dips to the WSW (Fig. 14d, e). When not parallel to the dykes, these shear zones splay out from the dykes and truncate the bench fabric in surrounding tonalites, then re-join the margins of other dykes and/or steeper shear zones along strike (Fig. 14e). Thus, they define an imbricate thrust system with flat-ramp geometries in the basement gneisses (Fig. 14a, b). Internal stretching lineations, sigmoidal lenses and asymmetric folds in basement-seated shear zones south of Svartbergan all support east- to ENE-directed thrusting (Fig. 12c), although normal drag of some mafic dykes into similar shear zones can be inferred locally (Fig. 14d). These low-angle basement-seated thrusts have the same orientation and kinematic character as the D_1 thrusts in metasedimentary units of the western foreland (Figs. 6, 7; see discussion).

The high-angle (steep) ductile shear zones striking NNW-SSE to NNE-SSW include the Olkeeidet shear zone in the west, and shear zones at Skarvatnet, Storvatnet, and Vannkista in south-central Vanna Island (Fig. 3). The Olkeeidet shear zone (Fig. 3) is traced southwards from the frontal Skipsfjord Nappe as the boundary fault to the western foreland metasedimentary sequence (Figs. 6, 7). In the north, this shear zone comprises an array of oblique, sigmoidal faults splaying outwards and merging back into the shear zone, defining a dextral strike-slip duplex. Southwards (Fig. 7) the Olkeeidet shear zone merges into and bounds a moderately west-dipping imbricate thrust system in the metasedimentary rocks (Fig. 10a, b). In small-scale, oblique-reverse faults and steep strike-slip faults with variable dip to the WSW classify the overall Olkeeidet shear zone as a combined thrust (in the south) and dextral-oblique strike-slip fault (in central part). In contrast, where the shear zone terminates against the Skipsfjord Nappe in the north (Figs. 3, 6), the gently NW-dipping foliation in the Skipsfjord Nappe rocks is bent sinistrally into the Olkeeidet shear zone (Fig. 11b-d). Stretching lineations on the moderate/steep shear zone at Skarvatnet (Fig. 3) plunge variable in the girdle, from WNW to SSW (Fig. 14 g, h). Combined with sigmoidal shapes of transposed carbonate clasts, this scatter indicates combined reverse (up-east) and sinistral strike-slip motion (see discussion).

In addition, most of the basement-seated shear zones on Vanna Island (Fig. 3) show hydrothermal alteration resulting in carbonate and quartz veins, breccias, and secondary albite, chlorite, and muscovite. Hydrothermal fluids have also caused local albitization in the surrounding host rocks and formation of fuchsite-rich schists.

4.5. Aeromagnetic data

New aeromagnetic data (Fig. 15) enabled us to separate metasedimentary units from the basement gneisses, mafic intrusive sills and dyke swarms, and Palaeoproterozoic ductile fabric trends (e.g. D_1-D_2 fabrics). The tonalitic basement and metasedimentary rocks in general are low- to non-magnetic, whereas mafic sills and dykes show up as semi-linear magnetic highs (Fig. 15a). Further, the displaced magnetic anomalies help to identify e.g. ductile shear zones, where a progressive displacement of the affected anomalies occurs, while brittle structures truncate abruptly the anomalies.

The magnetic anomaly patterns correspond well with the mapped basement-cover and foreland fold-thrust belt domains (Fig. 15; 1–4 domains). 1) The metasedimentary sequences in the western and southeastern foreland domains of the island are shown by markedly contrasting high and low magnetic responses (Fig. 15). These contrasts may be due to the strong magnetic response of the diorite sill intrusions, and low magnetic signature of the metasedimentary host rock. The different trends of presumed D_1 (NW-SE) and D_2 (NE-SW) structures are also well constrained, for example, where the Vanna Group contact cross-cuts NW-SE striking D_1 thrusts. 2) The more highly strained metasedimentary units of the Skipsfjord and Svartbergan Nappes show less contrast between diorite intrusions and metasedimentary host rocks, but evidently locate the allochthonous nappes well. This lack of magnetic contrast is likely due to the gentler dip of foliation and abundance of mafic sheets in the Skipsfjord Nappe. 3) Within the low magnetic massive basement tonalites of southern Vanna Island, variably N-S, NNW-SSE and NNE-SSW trending strong semi-linear magnetic anomalies exist, that reflect both the gentle and moderate west-dipping mafic dykes, the associated and closely linked thrusts, and the steep, ductile strike-slip shear zones. 4) A stronger magnetic signature is evident for basement rocks north of the Vannareid-Burøysund brittle fault, which is expressed as an NW-SE trending magnetic lineament (Fig. 15). This northern basement area, however, is beyond the scope of the present paper.

5. Discussion

5.1. Palaeoproterozoic basin sedimentation, architecture, and controlling factors

Previous studies in the WTBC show that Palaeoproterozoic (2.4–1.9 Ga) metasedimentary sequences were deposited on top of Neoarchaean

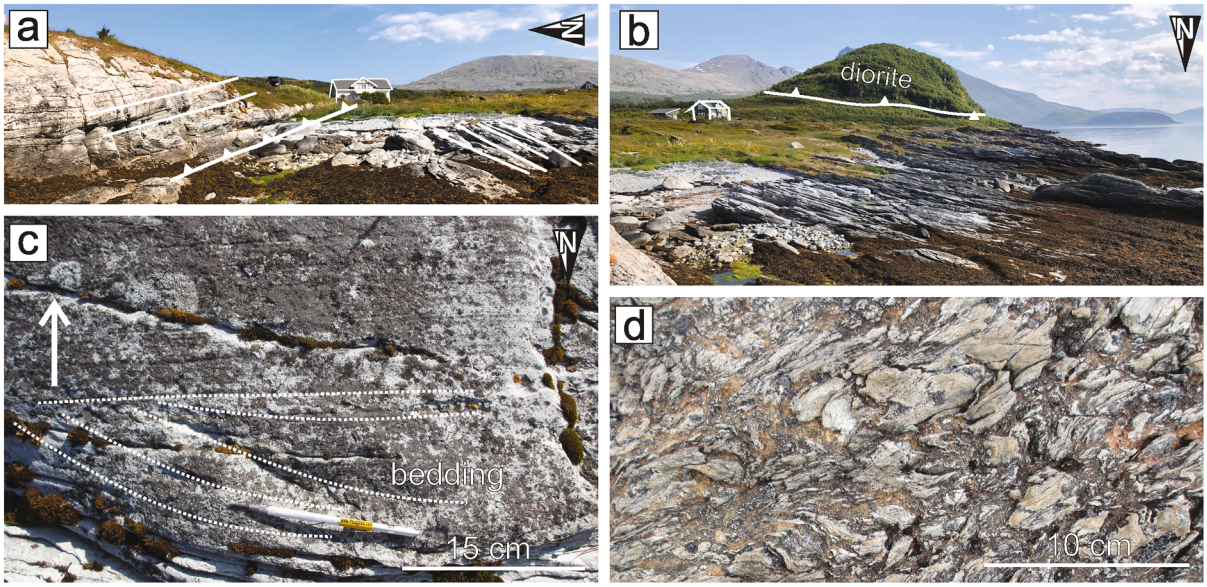

Fig. 8. Field photos showing lithologies and contact relations in the western foreland units, along shore north of Hamre (see Fig. 6). a) Frontal portion of the Skipsfjord Nappe thrusted over gently south-dipping metapelites (white lines on right side). The thrust fault and overlying metatonalites (white lines on the left side) dip to the NW. b) Shallow south-dipping foliation in metapelites near basement-cover contact. Note diorite sill in the hill (Hamreklubben), with thrust contact to the underlying metapelites. c) Relict trough cross-bedding in metasandstones near Hamre, indicating right way-up. d) Calcareous breccia with fragments of dismembered metapelite and metasandstone enclosed in a carbonate matrix.

tonalitic basement rocks and may have covered an extensive basin and/or several smaller basins (Bergh et al., 2010). The studied sequences on Vanna Island are in this paper further spatially separated and have varied depositional, thrust, and strike-slip boundary contacts to the basement tonalites (Fig. 3). Based on similarities in the established (this work) stratigraphic columns (Fig. 16) with the Vanna Group (Bergh et al., 2007) we interpret the metasedimentary cover rocks to represent correlative sequences deposited in separate intracontinental rift- and/or marginal basins, possibly linked through N-S and NE-SW trending depressions along transfer faults in between basement ridges (see below). The uniform successions of metapelite overlying metasandstones mark a primary fining-upward tendency, although internal thrusts may have repeated the sequences. The massive and laminated mudstones of the Bukkheia Formation, and similar lithologies in the western foreland (Fig. 16) suggest formation in subsiding basins as possible outer shelf deposits (cf. Clifton et al., 1971). Observed stratigraphic and thickness changes in the basal metasandstones (Fig. 16), and possibly remains of normal drag in basement-seated shear zones (Fig. 14d), suggest basin(s) bounded by normal faults striking N-S in the west, and NE-SW adjacent to the Vanna Group and Svartbergan Nappe farther east (Bergh et al., 2007), although kinematic evidence for normal faulting is generally lacking.

Correlation of the par-autochthonous cover units on Vanna Island with those of the allochthonous Skipsfjord and Svartbergan Nappes (Fig. 16) is more difficult due to the strong ductile shearing. However, supracrustal units in both nappes have quartzitic metasandstones at the base and an overlying pile of metapelites, now muscovite and calcareous schists. Further, metapelites in all areas are intruded by diorite sills. We therefore suggest a genetic relationship between the par-autochthonous and allochthonous foreland units, and that they were all part of the same Palaeoproterozoic basin succession.

The metasedimentary sequences on Vanna Island were deposited during a period when regional NE-SW extension occurred in the northern Fennoscandian Shield (Balagansky et al., 2001). These events marked an early rifting between c. 2.5–2.1 Ga, followed by a c. 2.1 Ga drifting and separation of the Archaean continent by new-formed oceans (Lahtinen et al., 2008, 2015; Bingen et al., 2015). These extensional events produced NW-SE trending rift basins bound by normal faults and elongate fault-bounded basement ridges (Lahtinen et al., 2008; Skyttä et al., 2019). Synchronously, voluminous mafic dykes and sills (c. 2.4 Ga and 2.2 Ga) intruded in the Archaean craton (Amelin et al., 1995) that stretched even beyond the region covered by the Caledonides and into Laurentia (Skyttä et al., 2019).

In the WTBC, at least one similar extensional pulse led to the intrusion of the 2.4 mafic dyke swarm that covers most of the islands from Senja to Vanna Island (Fig. 2; Kullerud et al., 2006). These mafic dykes generated weak zones in the basement tonalites that may have controlled the location and spatial extent of the Palaeoproterozoic basins. For example, in rift basins, the shape and topography of the paleocoastline would control the transport and extent of sedimentation, preferentially parallel to the rift axis and bounding normal faults (cf. Bergh and Torske, 1986, 1988). In the Tinnvatn Formation at Vikan c. N-S trending transport directions of the deltaic streams were determined (Johannessen, 2012), and were likely controlled by similarly oriented normal faults. A possible candidate for such a relict *syn*-rift normal fault is the NNE-SSW trending Olkeeidet shear zone, and many other c. N-S trending basement-seated ductile shear zones in southern Vanna Island (Fig. 3). The c. N-S trending mafic dykes in basement tonalites (Fig. 3) are mostly parallel to basement-seated D_1 thrusts and steep reverse and strike-slip faults (Fig. 14). Our interpretation is that these dykes intruded along *syn*-extensional normal faults that likely also bounded subsiding basin(s) as depo-centres for the Vanna Group and related sediments (Fig. 17a, 18a). The Olkeeidet shear zone may have originated as one of these extensional normal faults and later inverted as a combined reverse and strike-slip fault (see below). The widths of the extensional basins are unknown, but if the sediments formed as clastic shoreline deposits in rift basins, an undulating N-S trending rift axis could account for the arcuate shapes of the depositional basement cover contacts (Figs. 17, 18a). In addition, the post-deposition D_1-D_2 contractional events could have further modified the fault attitudes (see discussion below). Our results address the need for more detailed study of basement-seated shear zones and their kinematics to further constrain the geometry of the presumed normal fault network and the resulting extensional basin configuration.

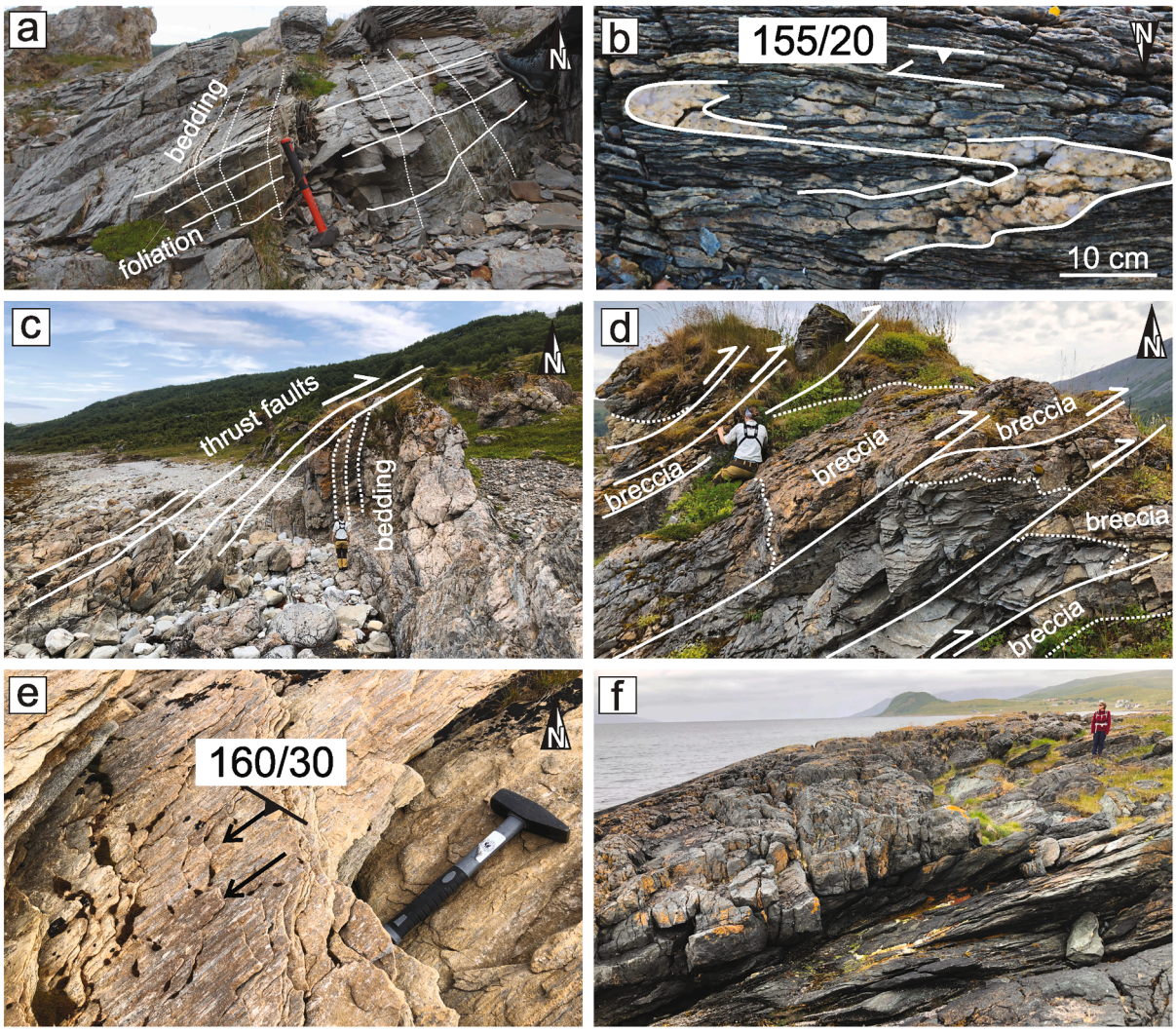

Fig. 9. Outcrop photographs of structural elements in the western foreland units at Hamre and Kvalvågklubben. a) Relict steeply east-dipping bedding (stippled lines) overprinted by a gently west-dipping foliation formed axial-planar to E-verging isoclinal folds. b) Intrafolial isoclinal fold within axial-planar mylonite fabric in metapelites, indicating top-to-ENE movement. c) Subvertical metasandstone beds (stippled lines) overridden by a gently west-dipping ductile thrust fault. Arrow indicates thrusting direction to the east. Locality between Solbakken and Finneset (see Fig. 7 for location). d) Carbonate breccia horizon (brown colour, bedding stippled white) in metapelites (dark grey) folded and transposed (white lines with arrows) into the main foliation. Note person for scale. e) Stretching lineations in metasandstones indicating top-to-ENE movement. f) Internal mylonitic thrust zone in diorite body at Svartneset (see Fig. 6 for location).

5.2. Basement-involved fold-thrust belt formation and basin inversion

5.2.1. D_1 fold-thrust belt propagation

We consider the rift basins and their presumed, c. NNW-SSE trending axis and bounding normal faults (Fig. 18a) to have controlled the extent and resulting geometry of the ENE-directed fold-thrust belt structures (D_1), and the corresponding inversion of metasedimentary units along steep N-S striking reverse shear zones (Figs. 17a, 18b). Such a control is based on overlap in attitude and location of low-angle D_1 thrusts relative to the steep, west-dipping reverse and strike-slip faults in basement rocks (Figs. 3, 16). We interpret the D_1 thrusts to have exploited the pre-orogenic low-angle mafic dykes and high-angle normal faults with dips to the west (Figs. 17a, 18a, b). This is confirmed by low-angle thrusts merging into the steep N-S strike-slip faults (Fig. 14d-f) creating a ramp-flat imbricate fault pattern, which indicates they formed separately and controlled the upward fault propagation. Such fault interaction is common both in thin-skinned fold thrust belts, where sedimentary strata control the thrust propagation (e.g. Boyer and Elliott, 1982), and in basement-seated belts where thrusts are detached above e.g. a low-friction deep crustal detachment and/or a frontal buttress (Lacombe and Mouthereau, 2002).

Mesoscale D_1 thrusts with flat-ramp and top-to-ENE propagation are common in the western foreland units (Fig. 9), where low-angle thrusts are localized to the axial surfaces of tight D_1 folds, and parallel to the main D_1 foliation both in the metasedimentary rocks and enclosed diorites. Thrust-ramps are interpreted where low-angle thrusts truncate steep, competent metasandstone beds in the footwall (Fig. 9c, d; cf. Jamison, 1987), and/or when they buttress against basement rocks as steep reverse and strike-slip faults (Figs. 11, 18b). This model is supported by the Olkeeidet shear zone (Fig. 10a, b) acting as a steep buttress against eastward transport of low-angle thrusts into the basement (Figs. 6, 7). Since most of the thrusts merge into such steep faults, they are temporally linked to the D_1 event.

Furthermore, if the steep normal faults became listric at depth, e.g. defining a pre-existing detachment, individual D_1 thrusts may have branched off the deep detachment and merged with a dyke or buttress at higher level in the basement, and thus controlled eastward thrust-ramp development. Similar thrust propagation is described in e.g. the Lewisian of Scotland (Tavarnelli, 1996; Butler et al., 2007).

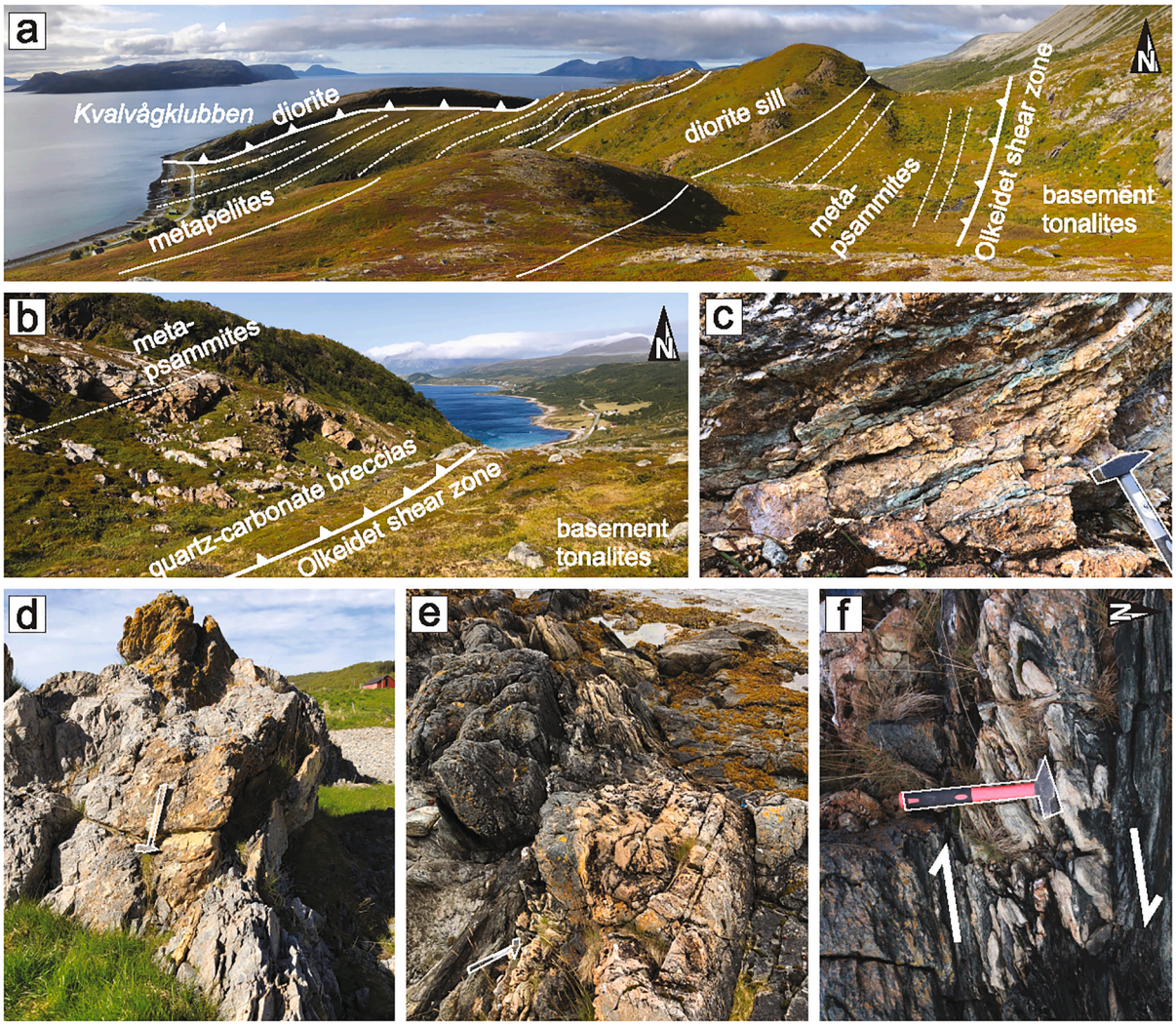

Fig. 10. Field photographs from the western foreland units showing architectures and structures related to diorite sills. a) W-E transect from Kvalvågklubben to Olkeeidet shear zone (Fig. 7), showing a diorite sill (centre of photo) in a west-dipping, imbricate thrust system (D_1), buttressed against the more steeply dipping, reverse Olkeeidet shear zone, that separates the metasedimentary sequence from the basement gneisses to the east. The diorite sill at Kvalvågklubben has a SE-directed thrust contact (D_2) and truncates the underlying metasedimentary units. b) Contact zone between Olkeeidet shear zone and metasedimentary units showing hydrothermal quartz-carbonate breccias (c. 30 m thick, brown-coloured rocks) in the hanging wall (west side). This breccia is traced intermittently along strike northward to Kvalvågen (see Fig. 7). c) Close-up view of the hydrothermal breccia in Olkeeidet shear zone, with coarse-grained carbonate (brown colour) and foliation-parallel green muscovite (fuchsite) layers cut by a network of quartz veins. d) Hydrothermal quartz-carbonate breccia (brown colour) in steeply dipping metapelites adjacent to the Olkeeidet shear zone at Kvalvågen. e) Hydrothermal quartz carbonate breccia associated with a steep ductile shear zone in the diorite at Solbakken (see Fig. 7). f) Isoclinal folds and transposed carbonate bands in the same steep ductile shear zone as in Fig. 10e (on horizontal surface), indicate dextral strike-slip movement.

5.2.2. D_2 fold-thrust belt propagation

The D_2 contractional event involved SE-directed folding and thrusting in the par-autochthonous Vanna Group (Fig. 4) in the south-east and thrusting of the allochthonous Skipsfjord and Svartbergan nappes in central Vanna Island (Fig. 3). D_2 structures are almost orthogonal to and superimposed on the NNW-SSE trending D_1 structures in southwestern Vanna Island. We argue for a two-phase model from refolding of D_1 folds and D_1 foliation by macro-scale D_2 folds (Fig. 6), truncation of D_1 fabrics by the Skipsfjord Nappe in the north, superposed folding at Larstangen and Myra in the southeast, and wider scatter in orientation of mineral and stretching lineations in the par-autochthonous units and Svartbergan Nappe than in the Skipsfjord Nappe. The latter addresses the possibility that D_1 structures also formed in the southeastern foreland and in the Svartbergan Nappe prior to SE-directed thrusting of the Skipsfjord Nappe, and/or be due to the contrasting D_1-D_2 tectonic transport directions.

The par-autochthonous Vanna Group, its enclosed diorite sill, and the basement-cover contact (Figs. 4, 17b, 18c) suffered D_2 progressive and coaxial tight folding followed by upright SE-vergent folding and thrusting (Fig. 5) due to c. NW-SE contraction. The repeated imbricate thrusts cutting up-section from the basement into the Vanna Group and diorite sills (Figs. 3, 4, cross-sections) suggest that the D_2 structures evolved from basement-involved thrust nappes to a thin-skinned foreland fold-thrust belt (cf. Boyer and Elliott, 1982). Imbricate thrust fans with supracrustal rocks occur mainly in the frontal parts of orogenic belts in contrast to more internal parts, where crystalline basement slivers are present and attached in duplex structures (cf. Morley, 1986; Vann et al., 1986).

The Skipsfjord Nappe is interpreted as an imbricate, foliation-parallel thrust system (Fig. 11a) with slivers of both basement and cover rocks. Uniform SE-directed shear senses suggest a similar, presumed progressive evolution as in the Vanna Group, thus advocating a temporal relationship. By contrast, the steep dip of strata in the Svartbergan Nappe could indicate formation in a basement-involved duplex

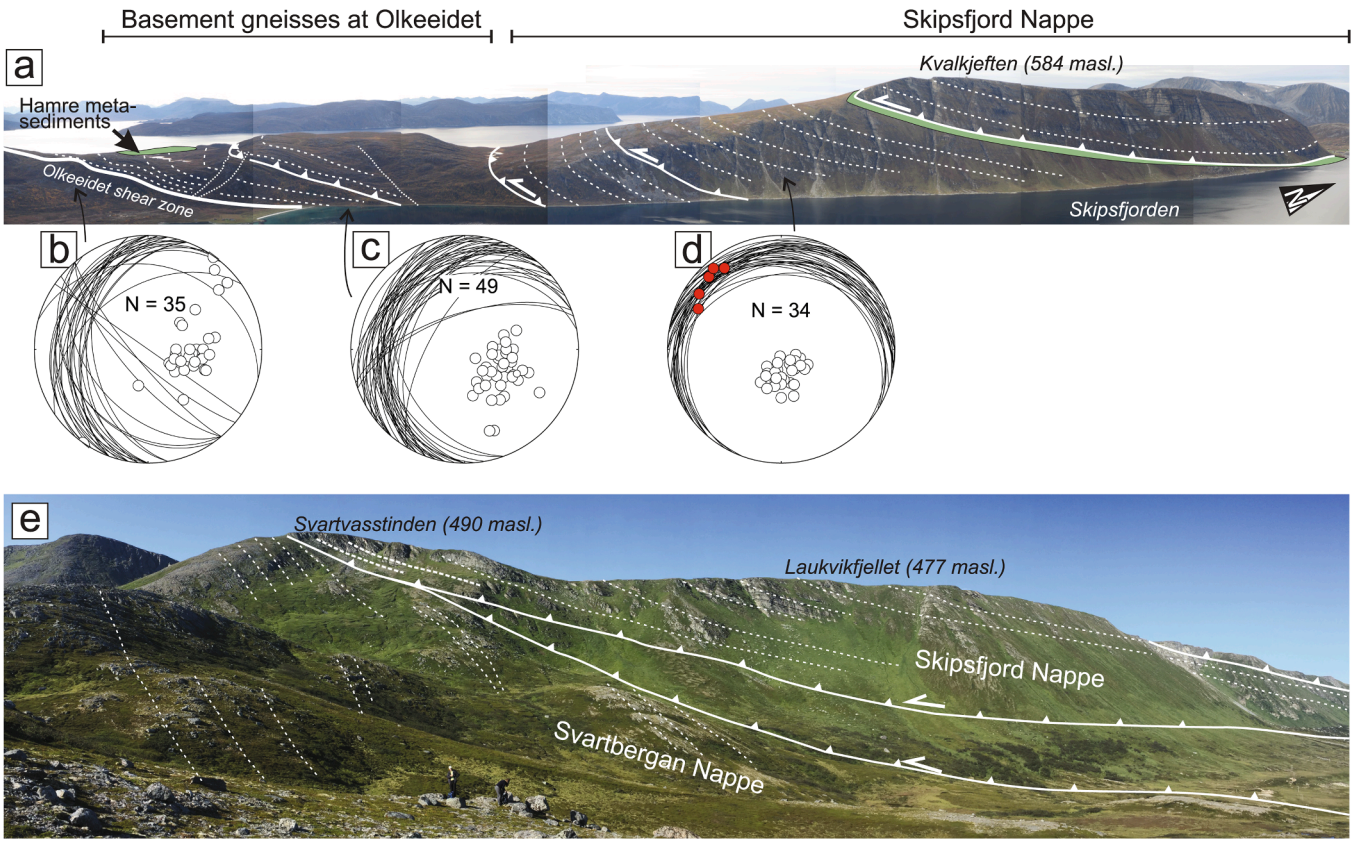

Fig. 11. a) Photographic cross section of the western part of the highly strained Skipsfjord Nappe. The gently north-dipping thrust sheets, with internal mylonitic fabrics (white stippled lines) include mafic intrusive layers sandwiched between imbricate slices of basement gneisses. The metasedimentary cover units (green coloured slices) mark the base of subsidiary thrust sheets. b, c, d) Equal-area lower hemisphere stereonets showing poles and great circles to foliation and stretching lineations. The foliation changes strike from N-S near Olkeeidet shear zone (left), via NE-SW in the basement gneisses just north of Olkeeidet, to E-W strike and gently N-dipping attitude in the Skipsfjord Nappe. e) Photographic cross section of the eastern part of the Skipsfjord Nappe and the underlying Svartbergan Nappe. Note steepening of the foliation to the south against the thrust contact with basement tonalites just outside the photo.

(e.g. Butler et al., 2007), in which the Skipsfjord Nappe defines the roof thrust system and the Svartbergan Nappe is a sliver bounded by steep, internal splay faults in the duplex behind a major NW-dipping thrust ramp (or buttress) (Figs. 12, 18c). Potential inverted buttresses could be pre-existing steep NW-dipping normal or *syn*-rift transfer faults, basement-cover contacts, and/or thick diorite sills as in the basin hosting the Vanna Group farther south, inferred by progressive upright refolding in the Vanna Group (Fig. 5c). Such basement and/or cover buttresses may then have acted as a stiff zone that tilted and partly inverted the strata in the Svartbergan Nappe, and in the Vanna Group, when they stepped upwards at a frontal thrust ramp (Fig. 18c). Similar architectures and propagating thrusts are known in modern collisional orogens with basement-involved fold-thrust belts (e.g. Butler, 1982; Gillcrist et al., 1987; Wibberley, 1997; Lacombe and Mouthereau, 2002), notably when basement sheets have been carried on a crustal-scale detachment from the hinterland to the foreland (cf. Nemčok et al., 2005).

If the Svartbergan Nappe stalled toward a basement ramp (Fig. 18c), the overlying Skipsfjord Nappe could have been thrusted SE-wards on top of and truncating the already stacked, steeply NW-dipping Svartbergan Nappe (Fig. 11e) along an out-of-sequence thrust (cf. Morley, 1988). Such faults, however, are more common in thin-skinned fold-thrust belts and require complete truncation of older, in-sequence fold-thrust structures (Butler, 1982; Morley, 1988). Our main argument is that rocks of the Svartbergan Nappe are steeply dipping, whereas the Skipsfjord Nappe units have gentle dip to the NW (Figs. 11, 12). Further, the Svartbergan Nappe rocks preserved an earlier-formed stretching lineation refolded by younger kink folds, whereas the Skipsfjord Nappe rocks only witnessed one uniform thrusting event, which would support out-of-sequence thrusting of the Skipsfjord Nappe.

The c. N-S striking steep reverse and dextral strike-slip faults like the Olkeeidet shear zone (Figs. 17, 18b) in the basement rocks are subparallel to the SE-directed translation of the Skipsfjord and Svartbergan Nappes during the D_2 event, and thus provided a favourable orientation for triggering continuous, orogen-parallel strike-slip reactivation (Fig. 17b, 18c). Sinistral movement is evident by bending of the frontal portion of the Skipsfjord Nappe inwards against the Olkeeidet shear zone (Figs. 6, 11, 17b, 18c). On a smaller scale, variably plunging and opposing stretching lineations in the shear zone at Skarvatnet (Fig. 14g, h) indicate reverse followed by sinistral strike-slip shear sense, and/or alternatively, may reflect the contrasting D_1-D_2 tectonic transport directions. Strike-slip faults with sinistral shear sense in the par-autochthonous Vanna Group and diorites south of Vikan (Fig. 4; Bergh et al., 2007), support D_2 sinistral strike-slip reactivation coeval with SE-directed thrusting.

We have argued for a spatial and temporal relationship between the allochthonous Skipsfjord and Svartbergan Nappes in the north and the fold-thrust belt in par-autochthonous Vanna Group units in the southeast (Figs. 3, 18c). In this D_2 orogen-parallel foreland transect, we emphasize the presence of a deep, basement-seated detachment in the north that merged up-section into flat thrust systems toward a buttress in the less deformed foreland in the southeast (Fig. 3; cross-section), in order to transfer orogenic contractional strain from deeper to shallower upper crustal levels (cf. Coward and Butler, 1985; Butler, 1986; Lacombe and Mouthereau, 2002). Furthermore, we state the role of pre-existing orthogonal normal and transfer faults, e.g. the presumed Olkeeidet

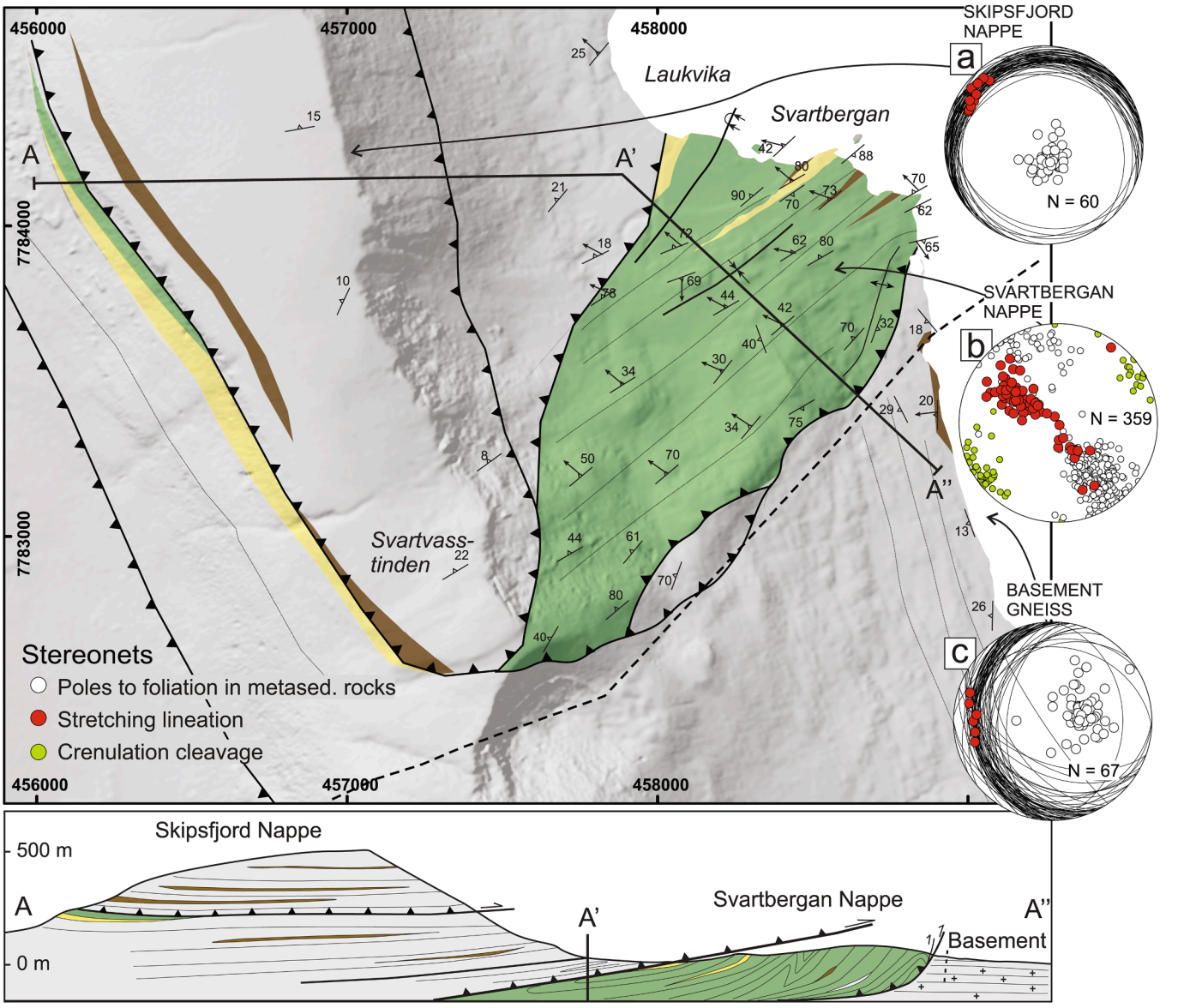

Fig. 12. Geological and structural map of the Svartbergan area. Legend as in Fig. 4. Cross-section A-A'' illustrates the transect across the Skipsfjord and Svartbergan Nappes toward the steep basement-cover (thrust) contact. Equal-area lower hemisphere stereonets showing poles and great circles to foliation, stretching lineations, and kink-fold hinges. Note that great circles in b) are removed for better visualisation. For location of map see Fig. 3.

shear zone and related strike-slip faults, to be more important than previously thought for strain localization, lateral segmentation, and partitioning of deformation during the late/post-Svecofennian D_1 and D_2 events, and in making barriers for thrust reactivation and inversion of the pre-existing basin sequences. The spatial distribution of such faults may, for example, explain why the western foreland units at Hamre-Kvalvågklubben largely escaped the D_2 strain.

5.2.3. *Shear zones and hydrothermal fluids*

Hydrothermal carbonate and quartz veins and chlorite-muscovite-fuchsite bearing alteration zones are common along the D_1 and D_2 basement-seated ductile shear zones on Vanna Island. These mineral assemblages suggest that fluids infiltrated along the shear zones and facilitated retrogressive, low-grade metamorphic alteration, preferentially due to thrusts propagating from lower to higher crustal levels during both the D_1 and D_2 fault movements. Whereas biotite and chlorite replaced amphibole and plagioclase in thrusts and strike-slip shear zones in mafic rocks, phyllosilicates dominate in mylonitic fault zones in the basement tonalites. Phyllosilicates in granitoid and tonalitic rocks generally make them weak (Wintsch et al., 1995), and faults rich in such aligned minerals can more easily permit hydrothermal fluid circulation, localize mineral occurrences, and exhibit aseismic slip. Increasing amounts of phyllosilicates in the shear zones may help to localize strain and leave the wall rocks relatively unstrained (Wibberley, 1999, 2005). Such processes may account for and explain why the D_1 ductile thrusts and steep strike-slip shear zones in the basement of Vanna Island became localized and further reactivated as orogeny-parallel strike-slip faults during D_2 deformation.

5.2.4. *Temporal constraints on the D_1-D_2 events*

Absolute timing of the D_1 and D_2 events on Vanna Island, and their relation to orogenic deformation farther south in the WTBC is uncertain. We favour a Palaeoproterozoic age for both events, where the D_1 event on Vanna Island represents the most peripheral part of the c. 1.77–1.75 Ga NE-SW shortening event (early-phase) in the WTBC hinterland (Bergh et al., 2010, 2015). By contrast, the orthogonal, SE-directed D_2 thrusting of the Skipsfjord and Svartbergan Nappes is interpreted as a result of progressive and/or partitioned orogen-parallel movement

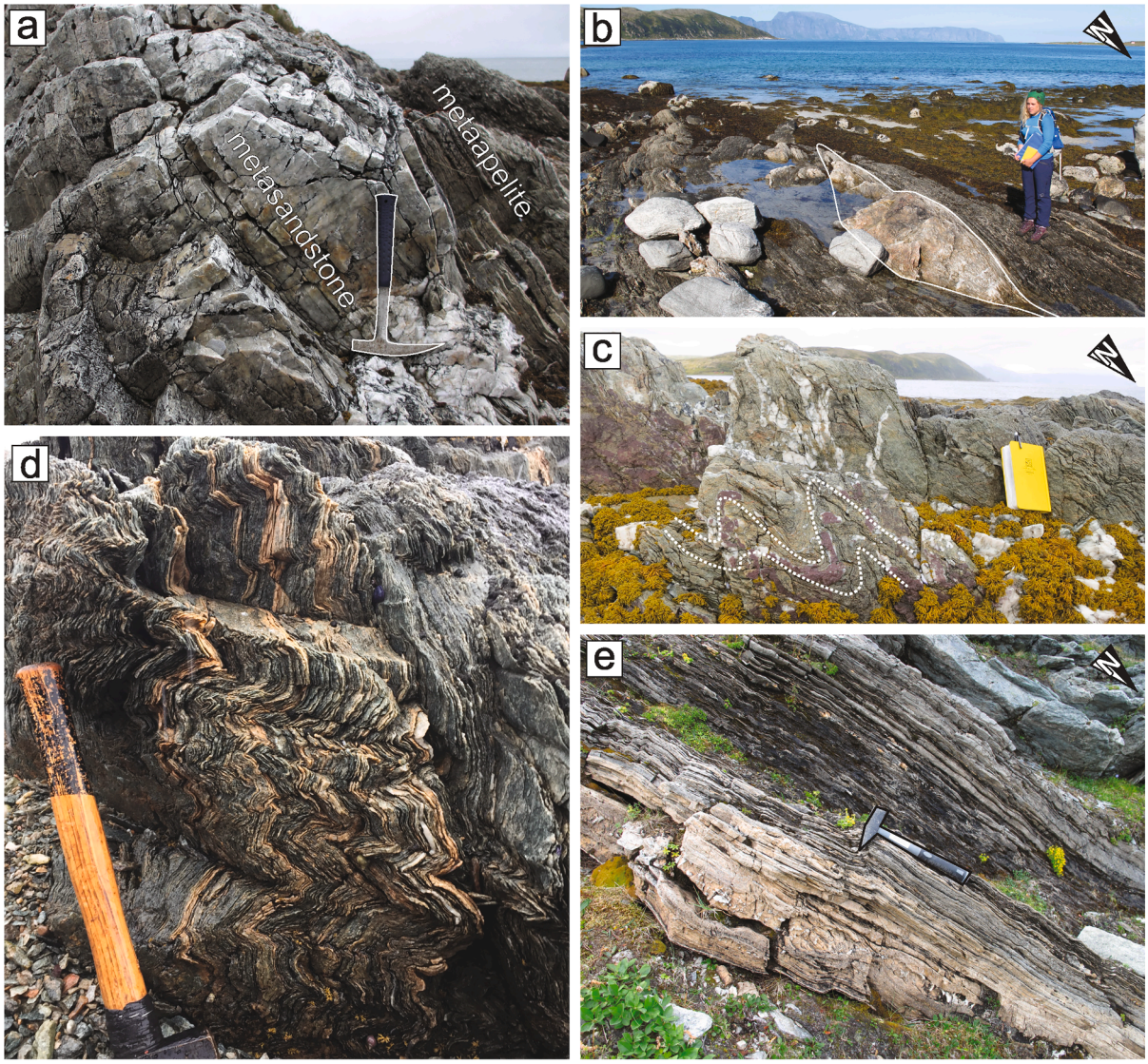

Fig. 13. Field photos of the Svartbergan Nappe lithologies and structures at locations seen in Fig. 12. a) Conformable, steeply dipping beds of metapelite and metasandstone at Laukvika. b) Lenses of basement tonalite within the metasedimentary sequence at Svartbergan. c) Small-scale, asymmetric, SE-verging folds likely representing parasitic folds to macroscale folding of the entire Svartbergan Nappe. Locality: shore at Svartbergan. d) Small-scale kink folding of subvertical metapelitic schists at Svartbergan. e) Mylonitic schists formed along the contact with the overlying Skipsfjord Nappe at Svartvasstinden.

(strain) in a setting with increased transpression in the foreland during the time interval c. 1.75–1.63 Ga, i.e. the late-stage event of Bergh et al., (2015). In support, we argue that the pre-existing c. N-S striking mafic dykes (2.4 Ga) and presumed basin-bounding normal faults (2.4–2.2 Ga?) provided favourable weak zones in the basement for orogen-normal and orogeny-parallel movements during D_1 and D_2 on Vanna Island. Similar steep ductile strike-slip shear zones also exist in the WTBC hinterland on Senja and Kvaløya (Fig. 2; Armitage and Bergh, 2005), formed at high/medium grade metamorphic conditions.

An alternative is that all the observed orthogonal structures (D_1-D_2) are the product of a single progressive deformation event with pronounced strain partitioning between the studied basin areas and bounding faults. One progressive evolution is, however, possible based on the similarity of fold-thrust belt geometries, mineral assemblages/low-grade metamorphism, and the character of the mineralization. But such a model is harder to document than our two-phase model based on the D_1-D_2 overprinting relationships argued for above. Thus, a fully partitioned model must await further detailed structural investigations, combined with radiometric age dating efforts.

Although Caledonian overprints in WTBC is generally absent (Corfu et al., 2003), preliminary ^{40}Ar-^{39}Ar dating of muscovite suggests a Caledonian age (c. 420 Ma) for the D_2 event in the Skipsfjord Nappe (NGU, pers. Comm., 2019). In our view, this age may represent a Caledonian reactivation of the Palaeoproterozoic thrust faults. Further dating is needed to resolve the significance of the inferred Caledonian ^{40}Ar-^{39}Ar age.

5.3. Regional comparison and implications

Palaeoproterozoic metasedimentary rocks (c. 2.4–2.2 Ga) as those on Vanna Island are present in the Alta-Kautokeino and Karasjok greenstone belts of northern Norway (Fig. 1; Siedlecka et al., 1985; Henderson et al., 2015). The Kautokeino Greenstone Belt has a basal fuchsite-bearing quartzite that hosts mafic sills dated at 2.22 Ga (Bingen et al., 2015), and overlain by mudstones and metasiltstones (Torske and Bergh, 2004) and corresponding metavolcanics. The youngest units are correlated with the Raipas Group at Alta (c. 2.15 Ga; Melezhik et al., 2015a) comprising well-preserved arkosic sandstones and associated calcareous mudstones (Zwaan and Gautier, 1980; Vik, 1985; Bergh and Torske, 1986, 1988; Melezhik et al., 2015a) and resembling the Vanna

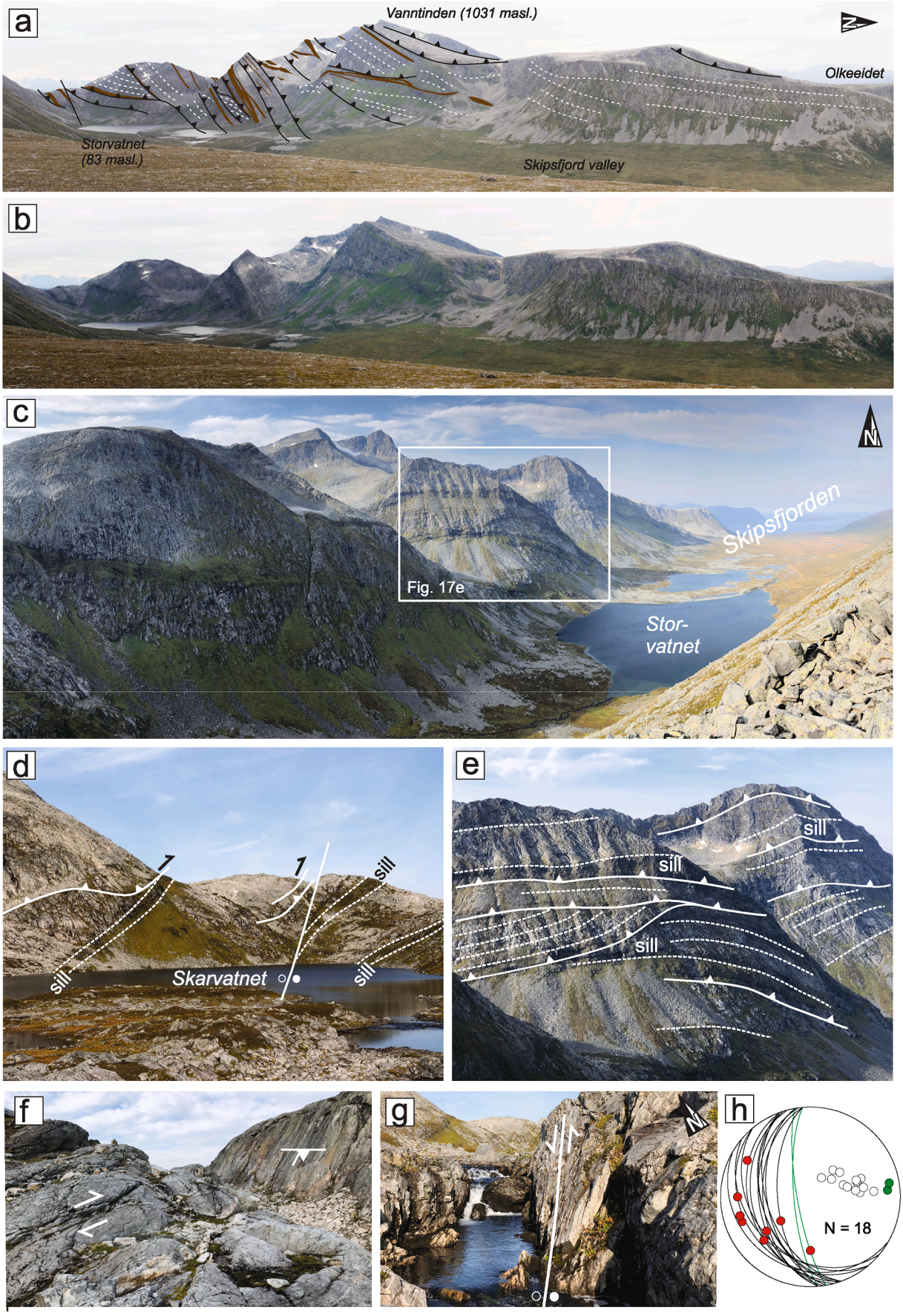

(caption on next page)

Fig. 14. Field photos of large- and small-scale features in basement tonalites in southern Vanna. a) Interpreted composite photographic cross-section through basement tonalites between Skarvatnet and Olkeeidet in southwestern Vanna (for location see Fig. 3). The massive tonalites have a bench fabric or weak foliation (white stippled lines) with sub-parallel mafic intrusive sheets (brown colour), and a fold- thrust belt system of imbricate, low-angle thrusts and subsidiary folds and associated high-angle strike-slip ductile shear zones trending c. N-S and with variable but mostly steep dip to the west (black lines with thrust symbols). b) Non-interpreted photo of a). c) Overview photo with view towards the north of basement rocks west of the Skipsfjord valley, showing intercalated bench fabrics, mafic sills, and low-angle (thrust) shear zones. d) Low-angle shear zones merging into mafic dykes and steeper, sinistral shear zones (heavy white lines). e) Close-up view of the steep mountainside at Storvatnet, where low-angle thrusts splay out from the mafic dyke contact and merge with steep strike-slip faults and mafic sill. Note internal truncations of bench foliation. f) Outcrops near the steep ductile shear zone in b. Low-angle shear zone fabrics (in foreground) merge with the steep reverse, sinistral shear zone (to the right). g) Exposed steep N-S trending ductile shear zone (as in b). Mineral lineations indicate sinistral movement. h) Equal-area lower hemisphere stereonets showing orientation data of the gently west-dipping shear zones with stretching lineations (red) showing dip-slip, up-to-NE motion and merging into steep ductile shear zone with sinistral strike-slip movement (green).

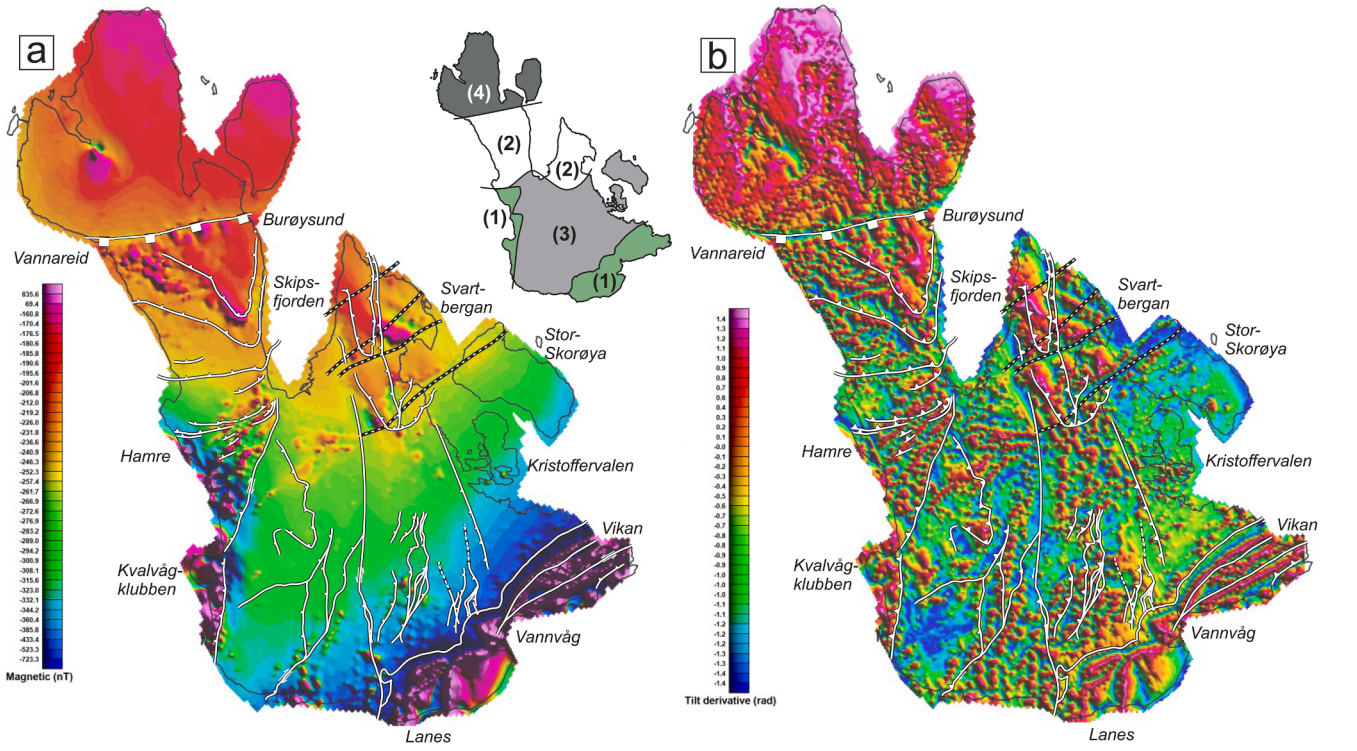

Fig. 15. Aeromagnetic data from the Geological Survey of Norway for Vanna Island show: a) total magnetic field and b) tilt derivative maps. Major ductile shear zones are shown in white and brittle faults are marked with a stippled black line. Small inset map shows the four main areas with distinct geophysical patterns discussed in the text.

Group. The Raipas Group sandstones are interpreted as tectonically induced fan deltas in an elongate N-S trending rift basin (Bergh and Torske, 1986, 1988). In terms of the long-lasting periods of Palaeoproterozoic extension (Skyttä et al., 2019), we consider the Raipas Group metavolcanic rocks to mark the onset of the major break-up of the Archaean craton at c. 2.1 Ga (Bingen et al., 2015), creating elongate rift basins filled by clastic and calcareous sandstones and mudstones, as on Vanna Island. Subsequently, the entire volcano-sedimentary Raipas Group succession was folded by E-W trending upright macrofolds during the Svecofennian E-W shortening (Henderson et al., 2015). At Alta, the macro-folds were refolded by SE-verging folds and cut by steep N-S trending strike-slip shear zones parallel to the bounding rift-basin faults (Henderson et al., 2015). Siliciclastic metasupracrustal rocks also exist in the Karasjok Greenstone Belt (Fig. 1; Often, 1985; Siedlecka et al., 1985; Braathen and Davidsen, 2000). Thick arkoses and fuchsite-rich quartzites with tentative ages of 2.22–2.06 Ga (Hansen et al., 2020) dominate, and have closely related metapelites and volcaniclastic deposits (Braathen and Davidsen, 2000). These rift-related clastic rocks were inverted and thrusted to the SW together with reworked Archaean basement rocks as fold-thrust nappes, likely during the Lapland-Kola Orogen (Krill, 1985; Marker, 1985).

The Karasjok Greenstone Belt can be traced southward into the Central Lapland Greenstone Belt and the Karelian Craton (Fig. 1; Patison, 2007). Rift-related greywackes and shelf deposits with mafic sills (c. 2.2–2.05 Ga) dominate in the Central Lapland (Hanski and Huhma, 2005; Huhma et al., 2018) and related Peräpohja, Kittilä and Kuusamo belts (Piippo et al., 2019; Lahtinen and Köykkä, 2020), and in the Norrbotten Province of Sweden (Bergman, 2018). These metasedimentary belts, possibly correlated with the WTBC and Kautokeino-/Karasjok greenstone belts, formed in a regional subsiding N-S trending rift basin system, and later on, were multiple deformed and inverted during the Svecofennian orogeny (Lahtinen and Köykkä, 2020). E-W shortening initiated at c. 1.93–1.90 Ga in the Kuusamo belt and resulted in an east-vergent foreland fold-thrust belt (Lahtinen and Köykkä, 2020). In the Peräpohja Belt, east to SE vergent Svecofennian inversion was controlled by two pre-orogenic orthogonal structures, i.e. a NW-SE trending graben system and E-W bounding normal faults (Piippo et al., 2019). Similarly, in the Norrbotten province (Fig. 1) N-S trending supracrustal basins (Bergman et al., 2001) record long-lived c. 2.2–2.1 Ga continental extension and mafic intrusions (Martinsson, 1997; Melezhik and Fallick, 2010; Lynch et al., 2018). In the Kiruna area these basins were inverted in response to first, a NE-SW crustal shortening at c. 1.88–1.87 Ga, then overprinted by E-W oblique shortening at c. 1.80–1.78 Ga and/or post-1.8 Ga (Lahtinen et al., 2018; Andersson et al.,

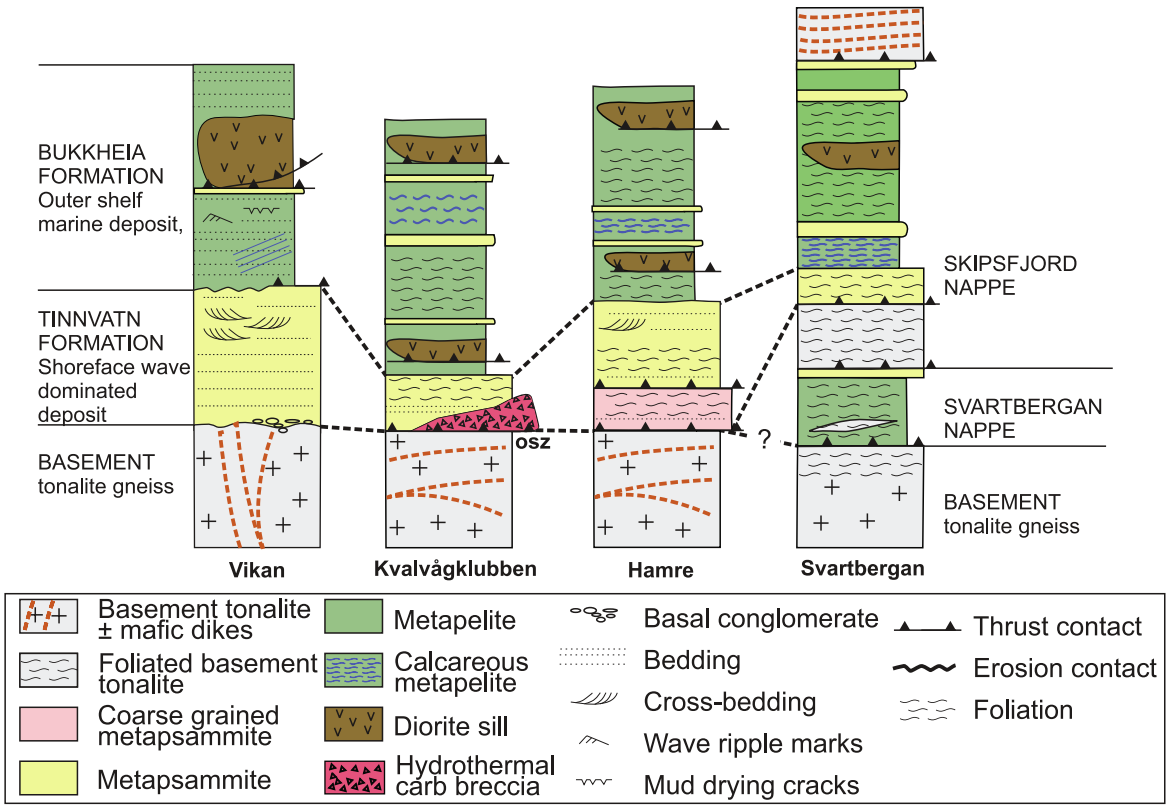

Fig. 16. Compilation of tectono-stratigraphic columns from Vikan (modified from Binns et al., 1980), Kvalvågklubben and Hamre areas (this study), and from the Skipsfjord and Svartbergan Nappes (this study; Opheim and Andresen, 1989) (see locations in Fig. 3). The columns show basement tonalites with overlying cover sequences. Note that columns are not to scale.

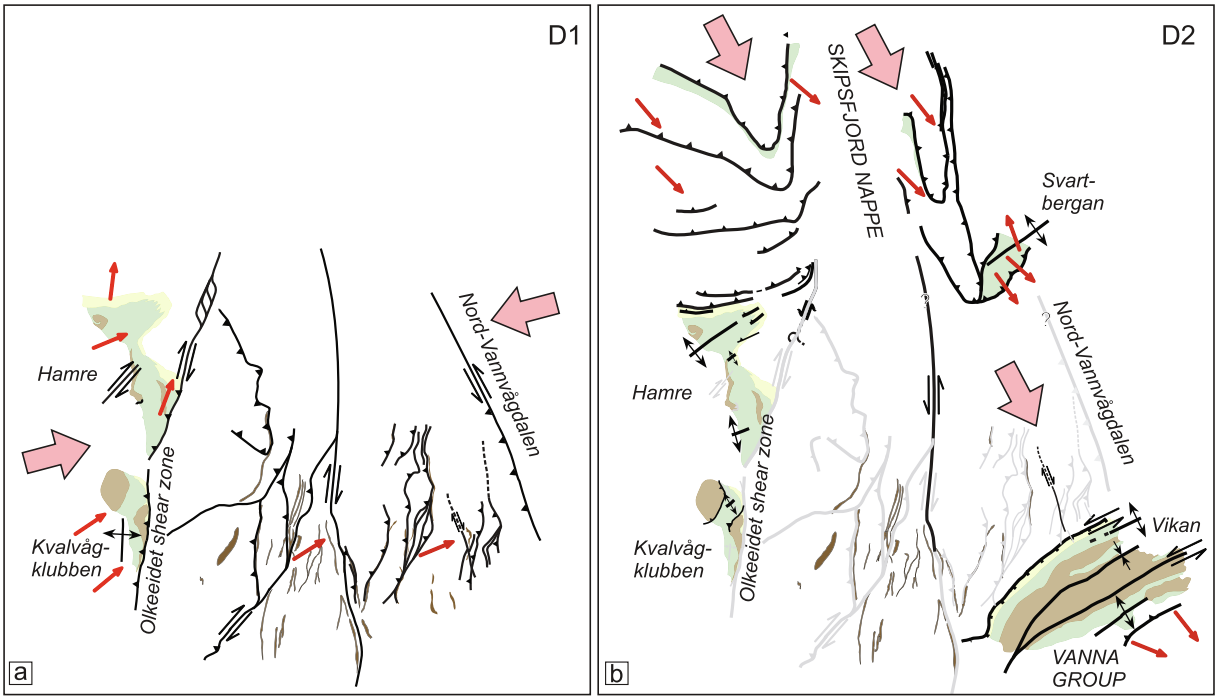

Fig. 17. Schematic model in map view of interpreted D_1 and D_2 structures at Vanna. a) D_1 event fold-thrust fabrics are located in the western and south-central parts of the Vanna foreland, both in metasedimentary strata (yellow = metasandstones, and green = metapelites), in basement tonalites, and along the boundaries of the mafic dykes (brown) in the basement rocks. The large pink arrows indicate ENE-WSW shortening direction, while small red arrows are thrust transport directions based on mineral and stretching lineations. b) D_2 event fold-thrust fabrics are associated with the Skipsfjord and Svartbergan Nappes, and with the Vanna Group in the southeastern foreland. Main shortening (large pink arrows) and thrust movement directions (small red arrows) are from stretching lineations. Note also refolding of the earlier D_1 folds and D_1 foliation in the western part of Vanna Island.

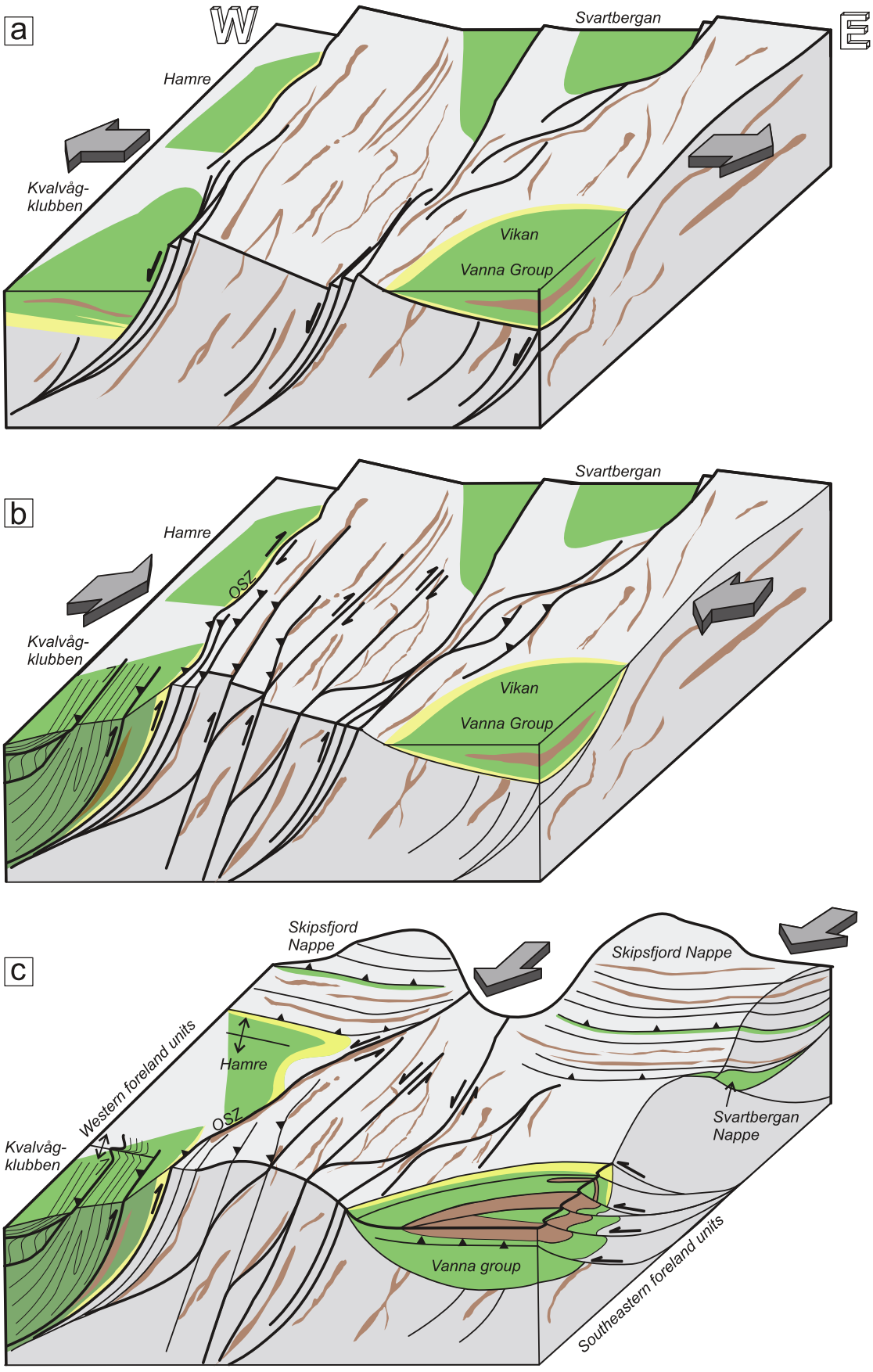

(caption on next page)

Fig. 18. 3-D model of the evolution of the Palaeoproterozoic (2.4–2.2 Ga) rift basins and late- to post-Svecofennian (c. 1.77–1.63 Ga) D_1-D_2 fold-thrust belt systems on Vanna. a) Formation of rift-related extensional basins on Vanna bounded by N-S trending, W and E dipping, listric normal faults. Such faults are located along 2.4 Ga intrusive mafic dykes trending similarly but with more gentle dips. b) D_1 inversion of the rift basins by ENE-WSW crustal shortening produced ENE-directed fold-thrust belt structures. Note ramp-flat geometry of west-dipping thrusts when they propagated from a potential basement-seated detachment at depth into low-angle mafic dykes, and as steep reverse faults when they buttress against steep normal and strike-slip faults (e.g. Olkeeidet shear zone - OSZ). c) D_2 fold-thrust structures formed by NW-SE crustal shortening. This shortening resulted in SE-vergent folding of the Vanna Group in the southeastern foreland, and SE-directed thrusting of the Skipsfjord and Svartbergan Nappes in the hinterland farther north. The earlier D_1 folds and foliation in the western foreland units at Hamre are refolded from N-S to NE-SW-trends, and steep N-S trending basement faults were reactivated as sinistral strike-slip faults. Note basement buttress in front of Svartbergan Nappe, and presence of one or two deeper detachment horizons ramping upward into the Vanna Group and against local buttresses of diorite sills.

2020), producing similar folds-thrust belts and partitioned lateral faults as during the D_1-D_2 events on Vanna Island.

These Fennoscandian fold-thrust belt forming events are, however, older than the early- and late phase shortening in the WTBC (and the D_1-D_2 events in Vanna Island). But they marked the onset of a long-lasting closure (Lapland-Kola orogen) of the Kola, Karelian, and Norrbotten cratons (Daly et al., 2006; Lahtinen et al., 2008) which likely, did not affect the WTBC in the time span after deposition (> 2.2 Ga) and the first deformation event in the WTBC (1.77 Ga). Thus, if the Vanna metasedimentary basins escaped both the Lappland- Kola and Svecofennian tectono-metamorphic shortening events, the 1.77–1.63 Ga deformation ages in WTBC are best explained by progressive westward younging of convergent tectonism toward the margin of the Fennoscandian Shield (Bergh et al., 2015). Alternatively, the WTBC could have been located in a different Archaean block or craton (i.e. Laurentia), and/or affected by comparable fold-thrust belt deformation styles later, i.e. during the Gothian orogeny (Bergh et al., 2015). Further age dating efforts are required to resolve these issues.

6. Conclusions

1) Metasedimentary sequences, now present as par-autochthonous and allochthonous fold-thrust belt units in the Vanna foreland, were deposited on top of Neoarchaean basement tonalites in pre-orogenic (2.4–2.2 Ga), N-S trending intracontinental rift- and/or shelf basins. Pre-existing mafic dykes (2.4 Ga) in the basement rocks acted as favourable weak zones that may have localized the Palaeoproterozoic rift basins and their bounding, steep west-dipping normal faults. The basins have similar internal stratigraphy with a lower series of metasandstones (arkoses) overlain by metapelites, calcareous breccias, and quartzites. Sedimentary structures and facies reconstructions indicate deposition in N-S trending, shallow-marine deltaic, tidal and/or shore face depositional environment.
2) The sedimentary cover units were folded and inverted along deep-seated thrusts and steep reverse faults by two orthogonal shortening events (D_1-D_2). The D_1 event suffered NE-SW shortening and formation of a basement-involved, NE-directed fold-thrust belt system linked to an early phase shortening in the WTBC hinterland. Pre-orogenic, west-dipping mafic dykes and basin-bounding normal faults became reactivated as thrust faults, steep reverse (buttress) and oblique, dextral strike-slip faults, thus enabling structural basement-cover inversion.
3) The D_2 event marked a switch to NW-SE-shortening with SE-directed thrusting of the Skipsfjord and Svartbergan Nappes in a basement duplex behind a NW-dipping thrust ramp (buttress), and associated SE-vergent fold-thrust deformation in the par-autochtonous Vanna Group. NW-SE trending D_1 structures were refolded into NE-SW-trends and cut by the D_2 nappes, and steep N-S trending basement faults reactivated as sinistral lateral faults contemporaneous with transpression and orogen-parallel movements in the WTBC farther west (1.75–1.63 Ga). Quartz-carbonate veins and fuchsite-schists are common in most of the D_1-D_2 related fold-thrust belt structures, advocating a strong structural control on hydrothermal fluid infiltration.
4) The fold-thrust belt architecture and structural relationships of the Vanna foreland is imaged well by high-resolution tilt-derivative aeromagnetic data. The data distinguish basement tonalites with mafic dykes, sedimentary units, basins and bounding faults, and enclosed diorite sills, and most important, separate D_1-D_2 trends of thrusts and basement-seated lateral ductile shear zones.
5) Comparison of the Palaeoproterozoic two-phase type (D_1-D_2) of foreland fold-thrust belt evolution on Vanna Island shows many similarities with rift-related sequences in Fennoscandia inverted by E-W to NE-SW shortening in, e.g. the Lapland-Kola and Svecofennian orogenic events, despite slightly contrasting ages of the deformation. Examples are the Alta-Kautokeino and Karasjok greenstone belts in northern Norway, the Central Lapland, Kittila, and Kuusamo greenstone belts of Finland, and belts in the Norrbotten Province of Sweden. The younger age of deformation in Vanna Island can be justified by progression of Svecofennian deformation westward or be due to early stages of the Gothian Orogeny.

CRediT authorship contribution statement

Hanne-Kristin Paulsen: Conceptualization, Visualization, Writing - original draft. **Steffen G. Bergh:** Conceptualization, Writing - review & editing. **Sabina Strmić Palinkaš:** Supervision. **Siri Elén Karlsen:** Investigation. **Sofie Kolsum:** Investigation. **Ida Ulvik Rønningen:** Investigation. **Paul E.B. Armitage:** . **Aziz Nasuti:** Data curation.

Declaration of Competing Interest

The authors declare that they have no known competing financial interests or personal relationships that could have appeared to influence the work reported in this paper.

Acknowledgements

This work was funded by UiT—the Arctic University of Norway as a part of the first authors PhD project. We thank two anonymous reviewers for constructive and thorough comments that improved the text considerably.

References

Åhäll, K.I., Connelly, J.N., 2008. Long-term convergence along SW Fennoscandia: 330 m.y. of Proterozoic crustal growth. Precambr. Res. 161, 452–474.
Amelin, Y.V., Heaman, L.M., Semenov, V.S., 1995. U-Pb geochronology of layered mafic intrusions in the eastern Baltic Shield: implications for the timing and duration of Paleoproterozoic continental rifting. Precambr. Res. 75, 31–46. https://doi.org/10.1016/0301-9268(95)00015-W.
Andersson, J.B.H., Bauer, T., Lynch, E.P., 2020. Evolution of structures and hydrothermal alteration in a Palaeoproterozoic metasupracrustal belt: Constraining paired deformation-fluid flow events in a Fe and Cu-Au prospective terrain in northern Sweden. Solid Earth 11, 547–578. https://doi.org/10.5194/se-11-547-2020.
Armitage, P.E.B., Bergh, S.G., 2005. Structural development of the Mjelde - Skorelvvatn Zone on Kvaløya, Troms: a metasupracrustal shear belt in the Precambrian West Troms Basement Complex, North Norway. Norw. J. Geol. 85, 117–133.
Balagansky, V.V., Timmerman, M.J., Kozlova Ye, N., Kislitsyn, R.V., 2001. A 2.44 Ga syntectonic mafic dyke swarm in the Kolvitsa Belt, Kola Peninsula, Russia: implications for early Palaeoproterozoic tectonics in the north-eastern Fennoscandian Shield. Precambr. Res. 105, 269–287. https://doi.org/10.1016/s0301-9268(00)00115-7.
Bauer, T.E., Skyttä, P., Hermansson, T., Allen, R., Weihed, P., 2014. Correlation between distribution and shape of VMS deposits, and regional deformation patterns, Skellefte district, northern Sweden. Miner. Deposita 49, 555–573.

Bergh, S.G., Corfu, F., Priyatkina, N., Kullerud, K., Myhre, P.I., 2015. Multiple post-Svecofennian 1750–1560 Ma pegmatite dykes in Archean-Palaeoproterozoic rocks of the West Troms Basement Complex, North Norway: geological significance and regional implications. Precambr. Res. 266, 425–439. https://doi.org/10.1016/j.precamres.2015.05.035.

Bergh, S.G., Corfu, F., Myhre, P.I., Kullerud, K., Armitage, P.E.B., Zwaan, K.B., Ravna, E. J.K., Holdsworth, R.E., Chattopadhya, A., 2012. Was the Precambrian basement of western Troms and Lofoten-Vesterålen in northern Norway linked to the Lewisian of Scotland? A comparison of crustal components, tectonic evolution and amalgamation history. Tectonics In Tech 11, 283–330. http://dc.doi.org/10.5772/48257.

Bergh, S.G., Kullerud, K., Armitage, P.E.B., Zwaan, K.B., Corfu, F., Ravna, E.J.K., Myhre, P.I., 2010. Neoarchean to Svecofennian tectono-magmatic evolution of the West Troms Basement Complex, North Norway. Norw. J. Geol. 90, 21–48.

Bergh, S.G., Kullerud, K., Corfu, F., Armitage, P.E.B., Davidsen, B., Johansen, H.W., Pettersen, T., Knudsen, S., 2007. Low-grade sedimentary rocks on Vanna, North Norway: a new occurrence of a Palaeoproterozoic (2.4-2.2 Ga) cover succession in northern Fennoscandia. Norw. J. Geol. 87, 301–318.

Bergh, S.G., Torske, T., 1988. Palaeovolcanology and tectonic setting of a Proterozoic metatholeiitic sequence near the Baltic Shield margin, northern Norway. Precambr. Res. 39, 227–246. https://doi.org/10.1016/0301-9268(88)90021-6.

Bergh, S.G., Torske, T., 1986. The Proterozoic Skoadduvarri sandstone formation, Alta, Northern Norway: a tectonic fan-delta complex. Sed. Geol. 47, 1–26. https://doi.org/10.1016/0037-0738(86)90068-0.

Bergman, S., 2018. Geology of the Northern Norrbotten ore province, northern Sweden. Sveriges Geol. Unders., Rapporter och meddelanden 141, pp. 430. ISBN 978-91-7403-393-9.

Bergman, S., Kübler, L., Martinsson, O., 2001. Description of regional geological and geophysical maps of northern Norrbotten County (east of the Caledonian orogen). Sveriges Geol. Unders. Ba 56, 110 pp.

Bingen, B., Solli, A., Viola, G., Torgersen, E., Sandstad, J.S., Whitehouse, M.J., Røhr, T.S., Ganerød, M., Nasuti, A., 2015. Geochronology of the Palaeoproterozoic Kautokeino Greenstone Belt, Finnmark, Norway: Tectonic implications in a Fennoscandia context. Norw. J. Geol. 95, 365–396.

Binns, R.E., Chroston, P.N., Matthews, D.W., 1980. Low-grade sediments on Precambrian gneiss on Vanna, Troms, Northern Norway. Nor. Geol. Unders. Bull. 359, 61–70.

Bond, R.M.G., McClay, K.R., 1995. Inversion of a Lower Cretaceous extensional basin, south central Pyrenees, Spain. In: Buchanan, J.G., Buchanan, P.G. (Eds.), Basin Inversion. Publ, Geol. Soc. Spec, pp. 415–431.

Boyer, S.E., Elliott, D., 1982. Thrust systems. Am. Assoc. Petrol. Geol. Bull. 66, 1196–1230. https://doi.org/10.1306/03b5a77d-16d1-11d7-8645000102c1865d.

Braathen, A., Davidsen, B., 2000. Structure and stratigraphy of the Palaeoproterozoic Karasjok Greenstone Belt, north Norway - regional implications. Norw. J. Geol. 80, 33–50. https://doi.org/10.1080/002919600750042663.

Butler, R.W.H., Bond, C.E., Cooper, M.A., Watkins, H., 2018. Interpreting structural geometry in fold-thrust belts: why style matters. J. Struct. Geol. https://doi.org/10.1016/j.jsg.2018.06.019.

Butler, R.W.H., Matthews, S.J., Morgan, R.K., 2007. Structural evolution of the Achnashellach Culmination, southern Moine Thrust Belt: testing the duplex model, In: Ries, A.C., Butler, R.W.H., Graham, R.H. (Eds.), Deformation of the Continental Crust: The Legacy of Mike Coward. Geol. Soc. London, Spec. Publ. 272, 103-120. https://doi.org/10.1144/gsl.sp.2007.272.01.07.

Butler, R., Tavarnelli, E., Grasso, M., 2006. Structural inheritance in mountain belts: an Alpine-Apennine perspective. J. Struct. Geol. 28, 1893–1908.

Butler, R.W.H., 1986. Thrust tectonics, deep structure and crustal subduction in the Alps and Himalayas. J. Geol. Soc. London 143, 857–873.

Butler, R.W.H., 1982. The terminology of structures in thrust belts. J. Struct. Geol. 4, 239–245. https://doi.org/10.1016/0191-8141(82)90011-6.

Cagnard, F., Gapais, D., Barbey, P., 2007. Collision tectonics involving juvenile crust: the example of the southern Finnish Svecofennides. Precambr. Res. 154, 125–141.

Clifton, H.E., Hunter, R.E., Phillips, R.L., 1971. Depositional structures and processes in the non-barred high-energy nearshore. J. Sed. Petrol. 41, 651–670. https://doi.org/10.1306/74d7231a-2b21-11d7-8648000102c1865d.

Corfield, S.M., Gawthorpe, R.L., Gage, M., Fraser, A.J., Besly, B.M., 1996. Inversion tectonics of the Variscan foreland of the British Isles. J. Geol. Soc. London 153, 17–32. https://doi.org/10.1144/gsjgs.153.1.0017.

Corfu, F., 2007. Multistage metamorphic evolution and nature of the amphibolite–granulite facies transition in Lofoten-Vesterålen, Norway, revealed by U-Pb in accessory minerals. Chem. Geol. 241, 108–128.

Corfu, F., 2004. U-Pb age, setting and tectonic significance of the anorthosite-mangerite-charnockite-granite suite, Lofoten-Vesterålen. Norway. J. Petrol. 45, 21. https://doi.org/10.1093/petrology/egh034.

Corfu, F., Armitage, P.E.B., Kullerud, K., Bergh, S.G., 2003. Preliminary U-Pb geochronology in the West Troms Basement Complex, north Norway: Archean and Palaeoproterozoic events and younger overprints. Nor. Geol. Unders. Bull. 441, 61–72.

Coward, M.P., Butler, R.W.H., 1985. Thrust tectonics and the deep structure of the Pakistan Himalaya. Geology 13, 417–420. https://doi.org/10.1130/0091-7613(1985)13<417:ttatds>2.0.co;2.

Cox, S.F., 2005. Coupling between deformation, fluid pressures, and fluid flow in ore-producing hydrothermal systems at depth in the crust. Econ. Geol. 100, 39–75.

Daly, S., Balagansky, V.V., Timmerman, M.J., Whitehouse, M.J., 2006. The Lapland-Kola orogen: Palaeoproterozoic collision and accretion of the northern Fennoscandian lithosphere, In: Gee, D.G., Stephenson, R.A. (Eds.), European Lithosphere Dynamics. Geol. Soc. Lond. Mem. 579-298. https://doi.org/10.1144/gsl.mem.2006.032.01.35.

Davids, C., Wemmer, K., Zwingmann, H., Kohlmann, F., Jacobs, J., Bergh, S.G., 2013. K-Ar illite and apatite fission track constraints on brittle faulting and the evolution of the northern Norwegian passive margin. Tectonophysics 608, 196–211. https://doi.org/10.1016/j.tecto.2013.09.035.

Eilu, P., Hallberg, A., Bergman, T., Feoktistov, V., Korsakova, M., Krasotkin, S., Kuosmanen, E., Livineko, V., Nurmi, P.A., Often, M., Philippov, N., Sandstad, J.S., Stromov, V., Tontti, M., 2008. Metallic mineral deposit map of the Fennoscandian Shield, 1:2 000 000. Geol. Surv. Finland, Geol. Surv. Norway, Geol. Surv. Sweden. The Federal Agency of use of mineral resources of the Ministry of Natural Resources of the Russian Federation.

Gaàl, G., Gorbatschev, R., 1987. An outline of the Precambrian evolution of the Baltic Shield. Precambr. Res. 35, 15–52.

Gillcrist, R., Coward, M., Mugnier, J.-L., 1987. Structural inversion and its controls: examples from the Alpine foreland and the French Alps. Geod. Acta 1, 5–35. https://doi.org/10.1080/09853111.1987.11105122.

Gorbatschev, R., Bogdanova, S.V., 1993. Frontiers in the Baltic Shield. Precambr. Res. 64, 3–21. https://doi.org/10.1016/0301-9268(93)90066-b.

Griffin, W.L., Taylor, P.N., Hakkinen, J.W., Heier, K.S., Iden, I.K., Krogh, E.J., Malm, O., Olsen, K.I., Ormaasen, D.E., Tveten, E., 1978. Archean and Proterozoic crustal evolution in Lofoten-Vesterålen. N Norway. J. Geol. Soc. London 135, 19. https://doi.org/10.1144/gsjgs.135.6.0629.

Hansen, H., Slagstad, T., Bekker, A., Bergh, S.G., 2020. Geochronology of the Karasjok Greenstone Belt establishes the ~2.22-2.06 Ga Lomagundi age for the Corgaš Formation carbonates with highly positive carbon isotope values. Abstract, Goldschmidt Seminar.

Hanski, E., Huhma, H., 2005. Central Lapland Greenstone belt. In: Lehtinen, M., Nurmi, P.A., Ramo, O.T. (Eds.), Precambrian Geology of Finland – Key to the evolution of the Fennoscandian Shield. Elsevier, Amsterdam, pp. 139–194.

Henderson, I., Viola, G., Nasuti, A., 2015. A new tectonic model for the Palaeoproterozoic Kautokeino Greenstone Belt, northern Norway, based on high-resolution airborne magnetic data and field structural analysis and implications for mineral potential. Norw. J. Geol. 95, 339–363. https://doi.org/10.17850/njg95-3-05.

Henkel, H., 1991. Magnetic crustal structures in northern Fennoscandia. Tectonophysics 192, 57–79. https://doi.org/10.1016/0040-1951(91)90246-o.

Homberg, C., Bergerat, F., Philippe, Y., Lacombe, O., Angelier, J., 2002. Structural inheritance and cenozoic stress fields in theJura fold-and-thrust belt (France). Tectonophysics 357, 137–158. https://doi.org/10.1016/S0040-1951(02)00366-9.

Hölttä, P., Balagansky, V., Garde, A.A., Mertanen, S., Peltonen, P., Slabunov, A., Sorjonen-Ward, P., Whitehouse, M., 2008. Archean of Greenland and Fennoscandia. Episodes 31, 13–19. https://doi.org/10.18814/epiiugs/2008/v31i1/003.

H. Huhma E. Hanski A. Kontinen J. Vuollo I. Mänttäri Y. Lahaye Sm–Nd and U-Pb isotope Geochemistry of the Palaeoproterozoic Mafic Magmatism in Eastern and 2018 Northern, Finland. Geol. Surv. Finland 150 Bulletin 405.

Jamison, W.R., 1987. Geometric analysis of fold development in overthrust terranes. J. Struct. Geol. 9, 207–219. https://doi.org/10.1016/0191-8141(87)90026-5.

Johannessen, H., 2012. Tinnvatnformasjonen i Vannas proterozoiske lagrekke: Sedimentære facies og avsetningsmiljø. Unpubl. MSc thesis. UiT The Arctic University of Norway, p. 105 pp..

Johansen, H., 1987. Forholdet mellom det prekambriske underlaget og overliggende sedimentære bergarter sør-øst på Vanna, Troms. Unpubl. Cand. scient thesis. UiT The Arctic University of Norway, p. 136 pp..

Kärki, A., Laajoki, K., Luukas, J., 1993. Major Palaeoproterozoic shear zones of the central Fennoscandian shield. Precambr. Res. 64, 207–223.

Karlsen, S.E., 2019. Strukturell og kinematisk analyse av Skipsfjorddekkets og underliggende bergarter i nordøstlige del av Vanna, Vest-Troms gneissregion. Unpubl. MSc thesis. UiT The Arctic University of Norway, p. 80 pp..

Knudsen, S., 2007. Strukturgeologi og petrologi i palaeoproterozoiske metasedimentære og intrusive bergarter på Vanna, Troms. Unpubl. MSc thesis. UiT The Arctic University of Norway, p. 113 pp..

Koistinen, T., Stephens, M.B., Bogatchev, V., Nordgulen, Ø., Wennerström, M., Korhonen, J. 2001. Geological map of the Fennoscandian Shield, scale 1:2 000 000. Geological surveys of Finland, Norway, Sweden, and the north-west department of ministry of Natural Resources of Russia.

Kolsum, S., 2019. Geometrisk og kinematisk analyse av duktile skjærsoner i metasedimentære og intrusive bergarter i Vannagruppen, Vest-Troms gneisregion, Troms, og deres relasjon til svekofenniske folde- og skyvestrukturer. Unpubl. MSc thesis. UiT The Arctic University of Norway, p. 86 pp..

Korsman, K., Koistinen, T., Kohonen, J., Wennerström, M., Ekdahl, E., Honkamo, M., Idman, H., Pekkala, Y. (Eds.), 1997. Bedrock Map of Finland 1:1000000: Finland. Geo, Surv.

Krill, A.G., 1985. Svecokarelian thrusting with thermal inversion in the Karasjok-Levasjok area of the northern Baltic Shield. Nor. Geol. Unders. Bull. 403, 89–101.

Kullerud, K., Skjerlie, K.P., Corfu, F., de la Rosa, J.D., 2006. The 2.40 Ga Ringvassøy mafic dykes, West Troms Basement Complex, Norway: the concluding act of early Palaeoproterozoic continental breakup. Precambr. Res. 150, 183–200. https://doi.org/10.1016/j.precamres.2006.08.003.

Lacombe, O., Mouthereau, F., 2002. Basement-involved shortening and deep detachment tectonics in forelands of orogens: insights from recent collision belts (Taiwan, Western Alps, Pyrenees). Tectonics 21, 1030. https://doi.org/10.1029/2001TC901018.

Lahtinen, R., Köykkä, J., 2020. Multiply deformed Paleoproterozoic foreland fold and thrust belt in northern Fennoscandia – the peripheral Kuusamo belt as a key example. Precambr. Res. 346, 105825 https://doi.org/10.1016/j.precamres.2020.105825.

Lahtinen, R., Huhma, H., Sayab, M., Lauri, L.S., Hölttä, P., 2018. Age and structural constraints on the tectonic evolution of the Paleoproterozoic Central Lapland Granitoid Complex in the Fennoscandian Shield. Tectonophysics 745, 305–325.
Lahtinen, R., Huhma, H., Lahaye, Y., Kousa, J., Luukas, J., 2015. Archean-Proterozoic collision boundary in central Fennoscandia: revisited. Precambr. Res. 261, 127–165. https://doi.org/10.1016/j.precamres.2015.02.012.
Lahtinen, R., Korja, A., Nironen, M., Heikkinen, P., 2009. Palaeoproterozoic accretionary processes in Fennoscandia. In: Cawood, P.A., Kröner, A. (Eds.), Earth Accretionary Systems in Space and Time. The Geological Society, London, pp. 237–256.
Lahtinen, R., Garde, A.A., Melezhik, V.A., 2008. Palaeoproterozoic evolution of Fennoscandia and Greenland. Episodes 31, 20–28. https://doi.org/10.18814/epiiugs/2008/v31i1/004.
Lahtinen, R., Korja, A., Nironen, M., 2005. Palaeoproterozoic tectonic evolution of the Fennoscandian Shield. In: Lehtinen, M., Nurmi, P.A., Rämö, T. (Eds.), The Precambrian Bedrock of Finland—Key to the Evolution of the Fennoscandian Shield. Elsevier Science B.V, Amsterdam, pp. 418–532.
Laurent, O., Auwera, J.V., Bingen, B., Bolle, O., Gerdes, A., 2019. Building up the first continents: Mesoarchean to Paleoproterozoic crustal evolution in West Troms, Norway, inferred from granitoid petrology, geochemistry and zircon U-Pb/Lu-Hf isotopes. Precambr. Res. 321, 303–327. https://doi.org/10.1016/j.precamres.2018.12.020.
Lynch, E.P., Hellström, F.A., Huhma, H., Jönberger, J., Persson, P.-O., Morris, G.A., 2018. Geology, lithostratigraphy and petrogenesis of c. 2.14 Ga greenstones in the Nunasvaara and Masugnsbyn areas, northernmost Sweden, In: Bergman, S. (Ed.), Geology of the Northern Norrbotten ore province, northern Sweden. Sveriges geol. Unders., Rapporter och meddelanden 141, 19-78. ISBN 978-91-7403-393-9.
Marker, M., 1985. Early Proterozoic (c. 2000–1900 Ma) crustal structure of the northeastern Baltic Shield: tectonic division and tectogenesis. Nor. Geol. Unders. Bull. 403, 55–74.
Martinsson, O., 1997. Tectonic setting and metallogeny of the Kiruna greenstones. Unpubl. PhD-thesis, Luleå University of Technology, p. 162.
Melezhik, V.A., Bingen, B., Sandstad, J.S., Pokrovsky, B.G., Solli, A., Fallick, A.E., 2015a. Sedimentary-volcanic successions of the Alta-Kvænangen Tectonic Window in the northern Norwegian Caledonides: multiple constraints on deposition and correlation with complexes on the Fennoscandian shield. Norw. J. Geol. 95, 245–284. https://doi.org/10.17850/njg95-3-01.
Melezhik, V.A., Solli, A., Fallick, A.E., Davidsen, B., 2015b. Chemostratigraphic constraints on the time of deposition of carbonate rocks in the Karasjok Greenstone Belt, northern Norway. Norwegian Journal of Geology 95, 299–314.
Melezhik, V.A., Fallick, A.E., 2010. On the Lomagundi-Jatuli carbon isotopic event: the evidence from the Kalix Greenstone Belt Sweden. Precambr. Res. 179, 165–190. https://doi.org/10.1016/j.precamres.2010.03.002.
Morley, C.K., 1986. A classification of thrust fronts. Am. Ass. Petrol. Geol. Bull. 70, 12–25. https://doi.org/10.1306/94885615-1704-11d7-8645000102c1865d.
Morley, C.K., 1988. Out-of-sequence thrusts. Tectonics 7, 539–561. https://doi.org/10.1029/tc007i003p00539.
Motuza, G., 2000. Description to the geological map of the central part of the Ringvassøya Greenstone Belt, Troms county, northern Norway. Report. Geol. Surv, Norw.
Myhre, P.I., Corfu, F., Bergh, S.G., Kullerud, K., 2013. U-Pb geochronology along an Archean geotransect in the West Troms Basement Complex, North Norway. Norw. J. Geol. 93, 1–24.
Myhre, P.I., 2011. U-Pb geochronology of crustal evolution and orogeny. Contributions from Caledonide Spitsbergen and the Precambrian West Troms Basement Complex, North Norway. Unpubl. PhD thesis, UiT The Arctic University of Norway. 125pp.
Nasuti, A., Roberts, D., Dumais, M.-A., Ofstad, F., Hyvönen, E., Stampolidis, A., Rodionov, A., 2015. New high-resolution aeromagnetic and radiometric surveys in Finnmark and North Troms: linking anomaly patterns to bedrock geology and structure. Norw. J. Geol. 95, 285–297.
Nemčok, M., Schamel, S., Gayer, R., 2005. Thrustbelts - structural architecture, thermal regimes and petroleum systems. Cambridge University Press.
Nironen, M., 1997. The Svecofennian Orogen: a tectonic model. Precambr. Res. 86, 21–44. https://doi.org/10.1016/s0301-9268(97)00039-9.
Often, M., 1985. The Early Proterozoic Karasjok Greenstone Belt, Norway: a preliminary description of lithology, stratigraphy and mineralisation. Nor. Geol. Unders. Bull. 403, 75–88.
Olesen, O., Lundin, E., Nordgulen, Ø., Osmundsen, P.T., Skilbrei, J.R., Smethurst, M.A., Solli, A., Bugge, T., Fichler, C., 2002. Bridging the gap between the onshore and offshore geology in Nordland, northern Norway. Norw. J. Geol. 82, 243–262.
Opheim, J.A., Andresen, A., 1989. Basement-cover relationships on northern Vanna, Troms Norway. Norsk geol. tidsskr. 69, 67–81.
Patison, N.L, 2007. Structural Controls on Gold Mineralisation in the Central Lapland Greenstone Belt, In: Ojala, J.V. (Ed.), Gold in the Central Lapland Greenstone Belt, Finland. Geo. Surv. Finland, Spec. Paper 44, 107-122.
Paulsen, H.-K., 2019. Structurally controlled hydrothermal mineralization: A case study from Vanna island, northern Norway. Unpubl. PhD thesis. UiT The Arctic University of Norway, p. 190 pp..
Paulsen, H.-K., Bergh, S.G., Palinkas, S.S., 2020. Late Palaeozoic fault-controlled hydrothermal Cu-Zn mineralization on Vanna Island, West Troms Basement Complex, northern Norway. Norw. J. Geol. 100, 1–41. https://doi.org/10.17850/njg100-1-2.
Pettersen, T., 2007. Strukturell analyse av metasedimentære bergarter på Vanna, Troms. Unpubl. MSc thesis. UiT The Arctic University of Norway, p. 112 pp..
Piippo, S., Skyttä, P., Kloppenburg, A., 2019. Linkage of crustal deformation between the Archaean basement and the Proterozoic cover in the Peräpohja Area, northern Fennoscandia. Precambr. Res. 324, 285–302.
Poblet, J., Lisle, R.J., 2011. Kinematic evolution and structural styles of fold-and-thrust belts. Geol. Soc. Spec. Publ. 349, 1–24. https://doi.org/10.1144/SP349.1.
Rodionov, A., Ofstad, F., 2012. Helicopter-borne magnetic, electromagnetic and radiometric geophysical survey at Vanna, Karlsøy, Tromsø. Geol. Surv. Norw, Report, p. 23.
Rønningen, I.U., 2019. Geometrisk og kinematisk analyse av paleoproterozoiske duktile skjærsoner i Skipsfjorddekkets undre del, Vanna, Vest-Troms gneisregionen, og relasjon til metasedimentære bergarter i Vannagruppen. Unpubl. MSc thesis. UiT The Arctic University of Norway, p. 110 pp..
Sandstad, J.S., 2015. MINN - mineral resources in North Norway. Norw. J. Geol. 95, 211–216. https://doi.org/10.17850/njg95-3-11.
Siedlecka, A., Krill, A.G., Often, M., Sandstad, J.S., Solli, A., Iversen, E., Lieungh, B., 1985. Lithostratigraphy and correlation of the Archaean and Early Proterozoic rocks of Finnmarksvidda and the Sørvaranger district. Nor. Geol. Unders. Bull. 403, 7–36.
Skyttä, P., Määttä, M., Piippo, S., Kara, J., Käpyaho, A., Heilimo, E., O'Brien, H., 2020. Constraints over the age of magmatism and subsequent deformation for the Neoarchean Kukkola Gneiss Complex, northern Fennoscandia. Bull. Geol. Soc. Finland 92, 19–38. https://doi.org/10.17741/bgsf/92.1.002.
Skyttä, P., Piippo, S., Kloppenburg, A., Corti, G., 2019. 2. 45 Ga break-up of the Archaean continent in Northern Fennoscandia: Rifting dynamics and the role of inherited structures within the Archaean basement. Precambr. Res. 324, 303–323. https://doi.org/10.1016/j.precamres.2019.02.004.
Tavarnelli, E., 1996. The effects of pre-existing normal faults on thrust ramp development: an example from the northern Apennines. Italy. Geol. Rundsch. 85, 363–371. https://doi.org/10.1007/bf02422241.
Torske, T., Bergh, S.G., 2004. The Čaravarri Formation of the Kautokeino Greenstone Belt, Finnmark, north Norway; a Palaeoproterozoic foreland basin succession. Nor. Geol. Unders. Bull. 442, 5–22.
Vann, I.R., Graham, R.H., Hayward, A.B., 1986. The structure of mountain fronts. J. Struct. Geol. 8, 215–227. https://doi.org/10.1016/0191-8141(86)90044-1.
Vik, E., 1985. En geologisk undersøkelse av kobbermineraliseringene i Alta-Kvænangenvinduet, Troms or Finnmark. Unpubl. PhD thesis. Geological Institute. NTH University of Trondheim, Trondheim, p. 295 pp..
Wibberley, C., 2005. Initiation of basement thrust detachments by fault-zone reaction weakening, In: Bruhn, D., Burlini, L. (Eds.), High-Strain Zones: Structure and Physical Properties. J. Geol. Soc. London, 347-372. https://doi.org/10.1144/gsl.sp.2005.245.01.17.
Wibberley, C., 1999. Are feldspar-to-mica reactions necessarily reaction-softening processes in fault zones. J. Struc. Geol. 21, 1219–1227. https://doi.org/10.1016/s0191-8141(99)00019-x.
Wibberley, C., 1997. A mechanical model for the reactivation of compartmental faults in basement thrust sheets, Muzelle region Western Alps. J. Geol. Soc. London 154, 123–128. https://doi.org/10.1144/gsjgs.154.1.0123.
Wintsch, R.P., Christoffersen, R., Kronenberg, A.K., 1995. Fluid-rock reaction weakening of fault zones. J. Geophys. Res. 100, 13021–13032. https://doi.org/10.1029/94jb02622.
Zwaan, K.B., 1989. Berggrunnsgeologisk kartlegging av det prekambriske grønnsteinsbeltet på Ringvassøya, Troms. Nor. Geol. Unders. Report 89, 101.
Zwaan, K.B., Gautier, A.M., 1980. Alta og Gargia. Beskrivelse til de berggrunnsgeologiske kart 1834 I og1934 IV. 1: 50 000. Nor. Geol. Unders. Skrifter 357, 1–47.